JOURNAL REVIEW

Spatiotemporal Patterns in Catalytic Reactors

Moshe Sheintuch and Stanislav Shvartsman
Chemical Engineering Dept., Israel Institute of Technology, Technion City, Haifa 32000, Israel

The study of spatial structures in heterogeneous reactors is a challenging academic topic, revealing patterns that differ from those known to exist in reaction-diffusion systems exposed to uniform conditions, as well as a practical problem that should affect design and operation procedures of commercial reactors like the catalytic convertor. Experimental observations and mathematical models of spatiotemporal patterns in high-pressure catalytic reactors are reviewed. Patterns in high-pressure reactors, in which thermal effects provide the positive feedback, as well as the long-range communication, usually emerge due to global interaction. Patterns are classified comprehensively by considering reactors of increasing degree of complexity: a wire or ribbon exposed to uniform conditions, a globally coupled catalyst in a mixed reactor or in a control loop, and a fixed bed in which interaction by convection occurs only in one direction. Catalytic wires are not expected to exhibit sustained patterns in the absence of global interaction. Global interactions by external control or gas-phase coupling are shown experimentally and analytically to induce a rich plethora of patterns. Complex motions were simulated to occur due to the interaction of convection, conduction and reaction in a fixed-bed; only a few of these patterns were experimentally observed. Directions for future research are suggested.

Introduction

Multiple steady states and periodic or aperiodic time-dependent solutions were demonstrated in numerous studies of catalytic and electrochemical reactions (see reviews by Sheintuch and Schmitz, 1977; Pismen, 1980; Razon and Schmitz, 1987; Hudson and Tsotsis, 1994; Ertl, 1990; Schuth et al., 1993; Imbihl, 1993; Slinko and Jaeger, 1994). While the interaction of diffusion and nonlinear kinetics is known to induce a plethora of spatiotemporal patterns, the identification of patterns observed in heterogeneous reactors is still ambiguous in many cases, partly due to experimental difficulties and nonuniformity of the system properties. The study of spatial structures in heterogeneous reactors is a challenging academic topic, revealing patterns that differ from those known to exist in reaction-diffusion systems exposed to uniform conditions, as well as a practical problem that should affect design and operation procedures of commercial reactors like the catalytic convertor. Oscillatory behavior has been observed during the oxidation of carbon monoxide, hydrogen, ammonia, hydrocarbons, alcohols, ethers, and formic acid, as well as during nitrogen monoxide reduction by ammonia or carbon monoxide and the hydrogenation of carbon monoxide or ethylene (see the previously cited reviews for citations of these oscillators). The catalytic convertor, as well as other pollution-abatement processes, employs noble-metal catalysts in order to oxidize carbon monoxide and hydrocarbons and to reduce nitric oxide to harmless products.

This work reviews experimental observations and mathematical models of spatiotemporal patterns in high-pressure catalytic reactors, along with the relevant analytical results and methods. While pattern formation is a classic problem of diffusion-reaction systems, and has been demonstrated in numerous studies of liquid-phase oscillators (e.g., the Belousov Zhabotinski reaction), pattern formation in high pressure-systems is distinctly different. In high-pressure reactors thermal effects provide the positive feedback as well as the long-range communication, and thermal patterns usually emerge due to the external control or the interaction of the catalyst with a mixed fluid phase. Our current understanding of catalytic oscillators suggests that they are governed by the interaction of a fast and long-range autocatalytic variable (typically, the temperature) with slow and localized changes in catalytic activity. Such one-dimensional systems are excitable but are unlikely to exhibit sustained spatiotemporal patterns

Correspondence concerning this article should be addressed to M. Sheintuch.
S. Shvartsman is currently at the Dept. of Chemical Engineering, Princeton University, Princeton, NJ 08544.

in the absence of global interaction. This review therefore focuses on the interaction of the fluid phase, through which the reactants are supplied, and the reactive solid phase. This interaction may produce patterns under conditions that, in the absence of such interaction, induce homogeneity in the catalyst phase. Experimentalists have tried to minimize this interaction by increasing the fluid flow rate into the reactor, or by applying control to the gas-phase concentration. This interaction may be significant even under these conditions, as evident from recent analysis (Levine and Zou, 1993; Mertens et al., 1993) of patterns observed by Ertl's group (see Lauterbach and Rotermund, 1994b, and Veser and Imbihil, 1994) during low-pressure oxidation of CO.

Heterogeneous reactors admit several other unique features that are described below:

- Heterogeneous reactors have a hierarchical structure: a catalytic site, a crystallite, a pore, a pellet, and a reactor. Each of these levels of organization may be assumed to be spatially homogeneous, while patterns appear only on a larger scale. Communication on a large scale is poorer, as certain species cannot diffuse: adsorbates may diffuse and transmit information only on a continuous-surface, gas-phase species diffuse only in the pore, or pellet and interpellet communication is limited to heat conduction. The dependence of the global dynamic behavior on the nature of the local dynamics (phase plane) repeats itself on various scales. The question that we would like to answer is the following: If each crystallite (or pellet) can exhibit bistability or oscillatory behavior, how many solutions and what patterns are possible for the pellet (or reactor)?
- Nonuniformity of properties, like catalyst loading and transport coefficients, are common to catalytic systems and cause ambiguity in the identification of many experimentally observed spatial patterns. Such nonuniformities occur not only because of technical difficulties but may arise naturally. The catalytic activity of edge and corner sites usually differs from that of regular surface sites, and defect sites may affect the behavior of the whole system. Recent observations made with a catalyst that exposes several crystal planes showed wave inception at the plane boundaries and their propagation through the surface; the system (a field emitter tip, which comprised several low-index crystal planes separated by plane boundaries) exhibited self-sustained oscillations, while the low-index single crystal always reached a steady state (Gorodetskii et al., 1994).
- Boundary conditions that apply to many heterogeneous reactors are different from the no-flux or fixed steady-state conditions commonly employed in models of reaction-diffusion patterns. While this difference may not be significant for patterns with a large wave number, most reported patterns in catalytic systems typically show one or few fronts.
- Many studies into complex dynamics or patterns employ external control aimed at maintaining constant (in time and *space*) operating conditions like temperature or reactant concentration. While the fluid phase is mixed and can, in principle, be controlled to attain such conditions, the solid phase cannot be mixed and control can be applied only to a spatially averaged property. That, in turn, may induce symmetry breaking and pattern formation.

These features apply to catalytic and electrochemical reactions as well as to gel or membrane reactors, which are currently used to study the BZ, the CIMA (chlorite-iodite-malonic acid) or other liquid-phase oscillatory reactions.

The scope and structure of the review are as follows: In the next section we write a general model that accounts for the fluid and solid phases and their interaction, in order to show how it differs from the classic reaction-diffusion model usually considered in the literature (Fife, 1979). The third section outlines the methodology employed here. In subsequent sections we present the main results of these models for common catalytic reactor geometries using three typical lumped characteristics kinetics: bistable, oscillatory, and excitable. We compare these results with those of simple reaction-diffusion systems and corroborate them, when possible, with experimental results. We do not elaborate on the detailed kinetics of bistable or oscillatory catalytic reactions. While the mechanism of oscillatory high-pressure reactions is still debated, it is clear that these instabilities are due to autocatalytic thermal effects, autoinhibition by a reactant, and slow reversible changes of catalytic activity. Several reviews of catalytic oscillatory kinetics under high pressure (Razon and Schmitz, 1987; Schuth et al., 1993; Slinko and Jaeger, 1994) as well as under low pressures (Ertl, 1990; Imbihl, 1993) are available. We do not review the magnificent patterns observed on single crystals at low pressures and fixed temperature, as those have been reviewed extensively (e.g., Imbihl, 1993); we cite a few such patterns, however, when they are accounted for by interaction with the fluid phase and have direct bearing on anticipated high-pressure patterns.

Heterogeneous Reactor Models

We write now a general heterogeneous model of a one-dimensional catalytic reactor and divide its description into three components: the fluid phase, the solid phase, and the nature of their interaction. Within each component we present several simple asymptotes and condense the information into a simple qualitative model that captures most of the features of the original model.

Fluid phase

The general fluid phase balance is a conventional axial-dispersion model of a reactor with heat and mass transfer resistance, except that we allow for a heat sink or a mass source (e.g., a cross-flow reactor), so that the fluid-temperature (T_f) or reactant concentration (C_{fi}) may not be monotonic. The balances typically account for accumulation, convection, axial-dispersion, transport to the solid phase, and heat loss by a coolant or by an endothermic reaction (at a rate of S_T) and reactant supply by transport through a membrane wall or by a preceding reaction (at a rate of S_C per unit reactor volume). Using conventional notation, the model can be written as

$$\epsilon_b T_{f,t} + V T_{f,z} - \frac{D_{eT}}{\rho C_{pf}} T_{f,zz} = -\frac{h A_V}{\rho C_{pf}} (T_f - T) - \frac{S_T(T_f, C_f)}{\rho C_{pf}}$$

$$\epsilon_b C_{fi,t} + V C_{fi,z} - D_{ei} C_{fi,zz} = -k_{ci} A_V (C_{fi} - C_i) + S_C(T_f, C_f) \tag{1}$$

subject to the conventional (Danckwerts) boundary conditions (Froment and Bischoff, 1990),

$$-D_{eT}T_{f,z}|_0 = V\rho C_{pf}(T_{\text{in}} - T_f|_0); \qquad T_{f,z}|_L = 0$$

$$-D_{ei}C_{f,z}|_0 = V(C_{i,\text{in}} - C_{fi}|_0); \qquad C_{f,z}|_L = 0, \quad (2)$$

where T is the solid-phase temperature and C_i is the concentration within the pores, or the boundary layer of the catalyst phase.

Mixing Asymptotes. The fluid phase balance can be reduced to several convenient forms that are considered in this review:

- *Plug-Flow Reactor.* When axial mixing is negligible, the fluid phase is described by the PFR equation ($D_i = 0$). Information is transmitted quickly downstream by convection, while upstream communication is limited to slow-moving fronts in the solid phase.
- *Mixed Reactor.* When mixing is good (or axial dispersion terms, D_{ej}/VL, are large), spatial gradients are negligible but the fluid phase properties differ from those of the inlet. The fluid-phase balance can then be integrated to obtain the CSTR asymptote

$$\epsilon_b T_{f,t} - \frac{T_f - T_{\text{in}}}{\tau_r} = -\frac{hA_V}{\rho C_{pf}}(T_f - \langle T\rangle) - \frac{S_T(T_f, C_f)}{\rho C_{pf}}$$

$$\epsilon_b C_{fi,t} - \frac{C_f - C_{i,\text{in}}}{\tau_r} = -k_{ci}A_V(C_{fi} - \langle C_i\rangle) + S_C(T_f, C_f), \quad (3)$$

where τ_r is the residence time and $\langle\,\rangle$ denote space-average properties of the solid phase.

- *Membrane Reactor.* When reactants are supplied and products and enthalpy are removed only through the reactor walls, while axial-flow is negligible ($V = 0$), the reactor may achieve a homogeneous solution at (T_f, C_f) values that nullify the right-hand sides of the enthalpy and mass balances. The dispersion terms are actually Fickian diffusion terms now. Note that this membrane-reactor asymptote is usually not considered in the reaction-engineering literature but, as we show, it can lead to stationary fronts and patterns.
- *Homogeneous Axial Dispersion Reactor.* This asymptote, which was a subject of extensive investigation in the 1970s and 1980s, applies when solid-to-fluid gradients are negligible (i.e., $T = T_f$ and $C_i = C_{fi}$) and the nonlinear reaction rate can be expressed in terms of the fluid variables $r(T_f, C_f)$. Its CSTR asymptote has been known to exhibit steady-state multiplicity and oscillatory behavior for many years now, while the plug-flow reactor (PFR) model cannot predict these behaviors. Steady-state multiplicity and oscillatory behavior can be predicted by the axial-dispersion model with a sufficiently large ratio of axial diffusion to convection terms (i.e., large $Pe = D_e/VL$); the existence of periodic motion requires also that the ratio of thermal and mass axial-dispersion terms be in a certain range (see Puszynski et al., 1981; Jensen and Ray, 1982a). We do not analyze the homogeneous model, but several reviews of these results are available (Hlavacek and Van Rompay, 1981). It is currently believed that this model cannot account for observations of catalytic oscillations, since instabilities have been observed on a single crystal, pellet, or wire even in the absence of interaction with the gas phase. Furthermore, for reasonable values of parameters the axial dispersion model predicts oscillations that are much faster than those observed experimentally. Recent analysis by Ivanova (1990) and Volodin et al. (1990) showed the variety of spatiotemporal behaviors in a two-dimensional slice of a fixed-bed reactor described by a homogeneous model. The recently suggested mechanism of DIFICI (differential-flow-induced chemical instability; Rovinsky and Menzinger, 1992) can be interpreted in terms of either a heterogeneous or homogeneous model, and is discussed below.

Thermal Asymptotes. The thermal balance can be reduced further to the following convenient forms:

- In an *adiabatic reactor* with a single reaction it is possible, under certain conditions (e.g., see Shvartsman and Sheintuch, 1995), to derive invariant relations between the fluid temperature and concentrations.
- When heat transfer to the reactor wall is good or when the fluid heat capacity is large, the fluid phase may be considered isothermal even under conditions when the solid- to fluid-temperature gradient is significant. Although this *isothermal-fluid* model has only rarely been considered in the literature, it is a limiting asymptote of the general non-isothermal heterogeneous-model of a catalytic reactor. While this asymptote may not readily apply to commercial-size reactors, it describes well laboratory reactors in which the fluid temperature is controlled to meet a certain setpoint. The isothermal-fluid reactor model was recently employed to account for moving-pulse patterns observed during hydrogen oxidation on a Ni-ring placed in a mixed-fluid reactor (Middya et al., 1994a; Graham et al., 1993b).
- When enthalpy effects are negligible, or heat removal from both phases is excellent, the reactor may be *truly isothermal.*

Solid phase

The solid-phase enthalpy balance accounts for accumulation, conduction, reactive heat generation, and transport to the fluid phase

$$\tau_T T_t - L_T^2 T_{zz} = \frac{(-\Delta H)r(T, C_i, \theta_i, \theta^*)}{ha_V} - (T - T_f) \quad (4)$$

subject to no-flux boundary conditions at its edges. The thermal relaxation temporal scale, $\tau_T = (\rho c_p)_s/ha_v$, is typically 1 s, in order of magnitude, and is much smaller than the characteristic time scale of the activation or deactivation processes. The latter determines the period of the oscillations. The characteristic thermal diffusion length in the solid phase, $L_T = (\lambda/ha_v)^{0.5}$, is much smaller than the reactor length. The rate depends on temperature (T) and on the fraction of active surface area (θ^*), as well as on reactant concentration at the surface (C_i) or at the absorbed layer (θ_i). The catalyst mass balances describe the change of concentrations within the catalyst pores or in the boundary layer adjacent to it. These balances are quite similar to the enthalpy balance

$$\tau_C C_t - L_C^2 C_{zz} = \frac{a_i r(T, C_i, \theta_i, \theta^*)}{k_c a_V} - (C - C_{fi}), \quad (5)$$

except that the diffusion term just cited is limited to intrapellet communication and cannot describe the interpellet mass transfer, unless the catalyst is in the form of a continuous washcoat. Typically, the mass-balance is established much faster than the enthalpy balance, while the diffusion length is smaller than the conduction length. Thus, if the solution to the mass balance is single valued, it may be substituted into the enthalpy balance. That may not be possible when $r(C)$ is not monotonic. The balances over the adsorbed species account for accumulation, diffusion—which is also limited to a continuous catalytic layer like a surface or a foil—and chemical reactions

$$\tau_\theta \theta_t - L_\theta^2 \theta_{zz} = f_i(T, C_i, \theta_i, \theta^*), \tag{6}$$

where f_i accounts for adsorption, desorption, and reaction steps. Again, this balance is of importance only when $f_i(T, C, \theta, \theta^*) = 0$ is multivalued within a certain domain of parameters.

The catalyst activity (θ^*) changes slowly. The nature of the slow variable, in general, has to be specified for each oscillator. For an extensive review of the chemistry of catalytic oscillators, see Schuth et al. (1993) and Slinko and Jaeger (1994). The mechanism of reversible oxidation and reduction of the surface has received most of the experimental support as the explanation of the slow step during oscillations under atmospheric conditions. The rates of oxidation and reduction of the catalyst are orders of magnitude lower than the rates of surface reactions (typically, seconds^{-1}), which explains the long oscillation periods and the time-scale separation. Nonnoble metals can undergo bulk oxidation and reduction, and for such systems changes in activity were attributed to changing oxidation states of the catalyst; Kurtanjek et al. (1980) measured the periodic variation of the work function during hydrogen oxidation on Ni catalyst. Amariglio et al. (1989) visually observed thermokinetic oscillations during propene oxidation on copper oxides: in the extinguished state the (red–orange) Cu_2O catalyzed partial oxidation, while in the ignited state the CuO (black) catalyzed complete combustion. Turner et al. (1981) proposed that reversible oxidation of the catalyst surface is responsible for oscillations during CO oxidation on noble metal catalysts. Oxide formation during this reaction was inferred from the *in-situ* IR study by Lindstrom and Tsotsis (1985) and from solid electrolyte potentiometry experiments (Vayenas et al., 1980). Recently, Hartmann et al. (1994), using *in-situ* X-ray, showed that silica-supported Pt clusters catalyzing CO oxidation underwent reversible oxidation to PtO/Pt_3O_4. The mechanism of surface reconstruction, which is well-established for oscillations on single crystals under low-pressure conditions, was ruled out. The smaller clusters were oxidized more readily. This may explain the observation that the existence of oscillations on supported catalyst depends on the particle size (Sant and Wolf, 1988). There is clearly a necessity of linking the well-established mechanisms of isothermal low-pressure oscillations, in which the slow step has been found to be either surface reconstruction (Ertl, 1990) or subsurface oxygen formation (Lauterbach et al., 1993; Lauterbach and Rotermund, 1994a), with the nonisothermal oscillations at atmospheric pressure conditions (see, e.g., Zhdanov, 1993). Obviously, the higher oxygen pressure accelerates the rate of surface oxidation. Reaction constants and activation energies that were determined at low pressures on single crystals cannot be simply extrapolated to high coverages and pressures since these parameters are coverage dependent.

In all the mechanisms presented earlier, the inhibitor—the fraction of the active surface area (θ^*)—is nondiffusing and the general form of its balance is

$$\theta_t^* = g(T, C, \theta_i, \theta^*). \tag{7}$$

The solid-phase model (Eqs. 4–7) describes a *catalytic wire, foil, or a fixed-bed* exposed to uniform gas-phase conditions (constant T_f, C_{fi}). In the nonisothermal model of exothermic reactions, surface temperature is likely to be the activator, while in its isothermal version it is the adsorbed species (θ_i). The inhibitor—the fraction of the active surface area (θ^*)—is nondiffusing. Spatial patterns are unlikely in such a one-dimensional reaction-diffusion system: The system may be excited to form traveling fronts or pulses, but they propagate out of the reactor which, in the absence of control or global interaction, eventually attains a uniform state.

Interaction

Pattern selection will be shown to be dominated by the interaction of the catalytic and fluid phases and the sequence of phase planes spanned in the reactor. The catalytic phase, which is in the form of a fixed-bed or a washcoat on the reactor wall, is mathematically similar to the wire problem, but the interaction with convection in the fluid phase introduces new motions and patterns. The fluid phase can be described by a CSTR or a PFR balance in its asymptotic case. We define the interaction to be *symmetry-breaking* (*symmetry-preserving*) if local ignition or extinction at one spot on the catalyst inhibits (accelerates) the same process in another one. The interaction in nonisothermal beds depends on the thermal regime. In an isothermal-fluid PFR, convection induces symmetry breaking in reactions with positive-order kinetics, while in adiabatic reactors convection inhibits asymmetry. When ignition occurs at the inlet of an isothermal-fluid reactor, it inhibits subsequent ignition of the outlet due to the declining concentration; ignition at the inlet of an adiabatic reactor will cause the fluid temperature to increase and that, in turn, will induce an ignition process downstream. In an isothermal bed, in which an oscillatory $A + B \rightarrow P$ reaction occurs, the interaction is symmetry preserving when the limiting reactant is rate inhibiting, while when a rate-accelerating reactant is limiting, the system tends to break the symmetry (see the analysis by Shvartsman and Sheintuch, 1994). Similar rules of interaction apply to gas-phase coupling in a mixed reactor (Middya et al., 1994a).

Condensed models

The model just outlined is too complex for qualitative analysis, and below we derive a minimalistic model that captures the main features of the detailed model. Such models have been extensively used to study nonlinear dynamics, and they capitalize mainly on universal behavior of the system in the vicinity of the Hopf bifurcation point (the Ginzburg–Landau equation) or on large separation of time and length scales.

We opt for the latter presentation, which describes well many catalytic oscillators and which may admit propagating front or pulse solutions. As we argued, many catalytic reactors can be described by a single gas-phase variable (denoted by λ below), a single autocatalytic variable (activator, u), and a slowly-changing ($\epsilon \ll 1$) and localized inhibitor (v). The condensed model takes the form

$$\gamma\lambda_t + U\lambda_z - \delta\lambda_{zz} = g(u) \tag{8a}$$

$$u_t - u_{zz} = f(u, v, \lambda) \tag{8b}$$

$$\frac{1}{\epsilon} v_t = h(u, v), \tag{8c}$$

Typically, λ is the fluid temperature in an adiabatic reactor or the fluid concentration in an isothermal reactor; $g(u)$ is a certain rate law that depends on the state of the surface, and U is a properly scaled fluid-velocity. No-flux boundary conditions apply to Eq. 8b while the Danckwert's conditions apply to Eq. 8a. The temporal and spatial coordinates have been rescaled so that the activator time and length scales are unity. Typically, $\gamma \ll 1$, as the fluid heat-capacity, is much smaller than that of the gas, and a pseudo-steady-state assumption can be invoked. The autocatalytic nullsurface, $f(u, v, \lambda) = 0$, should be fold- or cusp-shaped, while $g(u)$ and $h(u, v)$ may be monotonic; for the sake of simplicity we ignore the dependence of g on λ and y and of h on λ.

The fluid-phase model (Eq. 8a) can be reduced to the asymptotic forms of the PFR ($Pe = \delta/UL \to 0$), membrane reactor (MR) ($U = 0$), and CSTR ($Pe \to \infty$) models. In the latter case the fluid is assumed to be well mixed, but the catalyst state is distributed. When the CSTR residence time is small, the fluid-phase balance can be written as $U(\lambda_{in} - \lambda) = \langle (g(u)) \rangle L$, where $\langle\ \rangle$ denotes a space-averaged value, or

$$\lambda = (L/U)(g_0 - \langle g(u) \rangle), \tag{9}$$

with $g_0 = \lambda_{in} U/L$. The solid phase is described by Eqs. 8b and 8c. In typical reactor problems there exists a linear relation between the fluid variable and $\langle u \rangle$. Middya et al. (1994a) derived such a linear relation for an adiabatic or an isothermal-fluid reactor. They have analyzed the patterns possible in the asymptote of large ratio of catalyst volume to flow rate (infinite L/U), as well as patterns that emerge when L/U is finite; the system is stable when $L/U \to 0$. The case of infinite L/U is identical to that of an external control that maintains a catalyst at $\langle g(u) \rangle = g_0$ by varying λ. The patterns emerging in a controlled catalytic ribbon, which has been a subject for extensive investigation, are anticipated to emerge also in a catalytic reactor with a mixed gas-phase. Note that in both PFR and CSTR cases (when $\gamma \ll 1$) it is possible to convert Eqs. 8a and 8b into a single integrodifferential equation.

Recently, Rovinski and Menzinger (1992, 1993) suggested the following condensed model to describe convection-diffusion-reaction plug-flow systems

$$u_t - Uu_z - u_{zz} = f(u, v) \tag{10a}$$

$$\frac{1}{\epsilon} v_t = h(u, v), \tag{10b}$$

This simpler model assumes that the activator solid to fluid gradients are negligible, an assumption that does not usually apply to high-pressure catalytic reactors, but may apply to a bed catalyzing the BZ reaction. This model admits a homogeneous solution and the main results of its linear stability analysis and numerical simulations will be presented in the PFR chapter.

Methodology

We organize the results according to the reactor geometry: a catalytic wire or ribbon, a disc or foil, a distributed catalyst within a CSTR and a packed bed. The first two geometries are described by one- and two-dimensional reaction-diffusion equations for which the theory is well developed. Within each geometry we study the results for a single-variable bistable model before analyzing the motion of two-variable systems with bistable, oscillatory, or excitable kinetics. Within each kinetic regime we review the relevant analytical results, the experimental observations, and the ensuing mathematical models.

We do not discuss in detail the experimental methodology employed in the study of spatiotemporal concentration and thermal patterns. Monitoring spatiotemporal patterns is a complex experimental task since these patterns are not amenable to visual inspection, as in the BZ and other liquid-phase oscillators. Color changes have been employed for monitoring spatiotemporal patterns during iron electrodissolution (Hudson et al., 1993) and for following thermokinetic oscillations during propene oxidation on copper oxide catalyst. The observation of a glowing Pt wire during ammonia oxidation was used to follow the front motion (Barelko et al., 1978). Thermal patterns in catalytic reactors have long been monitored by an array of thermocouples (e.g., Kapicka and Marek, 1989; Onken and Wolf, 1988; Jaeger et al., 1986) or by a moving thermocouple in a thermowell (Adaje and Sheintuch, 1990). Thermocouple probing is satisfactory for portraying one-dimensional large-scale patterns (as in the fixed-bed, Dvorak et al., 1993), but will not give a coherent picture in two-dimensional systems and cannot be used for small-scale measurements or thin wires (Chen et al., 1993; Cordonier and Schmidt, 1989). Kaul and Wolf (1984) used the Fourier transform infrared (FTIR) spectrometry to study the propagation of ignition/extinction fronts during CO oxidation on supported Pt catalyst by measuring the IR spectra of selected areas of the surface.

The recent progress in the study of catalytic patterns is mainly due to the successful development of spatially resolving methods like IR thermography and photoelectron emission microscopy (PEEM). The first report on IR imaging of catalytic reactions was made by the group of Schmitz (see Brown et al., 1985, for the description of the experimental setup). The imaging system uses IR-sensitive semiconductor (InSb in the latter report) and achieves a spatial resolution of ~ 0.1 mm. IR thermography was successfully applied to study thermal patterns on supported catalysts, in the forms of wafers and pellets (Brown, 1985; Kellow and Wolf, 1990, 1991), as well as on catalytic ribbons and disks (Lobban et al., 1989; Lobban and Luss, 1989). Since the beginning of the 1990s, PEEM has been the major tool for studies of spatiotemporal patterns of catalytic reactions at pressures below 10^{-4} mbar

(Rotermund, 1993). The PEEM image is formed due to the work function differences of catalyst areas covered by different adsorbates: oxygen-covered areas look darker than the CO-covered areas since chemisorbed oxygen causes larger increase in the work function than CO. The spatial resolution attainable with PEEM is 0.2 μm. The method has been useful for the discovery of patterns during oscillatory CO oxidation on the Pt(110) plane. This method, unlike the scanning low energy electron diffraction, does not require well-ordered single-crystal surfaces for its applications and was successfully applied in dynamic studies on polycrystalline catalysts (Lauterbach and Rotermund, 1994b).

We emphasize the analysis and review of spatially continuous (as opposed to discrete) models, since the size of the experimental system and even the characteristic length of the pattern are usually large enough to warrant the use of partial differential equations. Some analytical results and qualitative understanding can be obtained by considering the behavior of systems with a wide separation of time or length scales, which are conditions that apply to many catalytic systems. Cell models, which account for an array of coupled units (such as sites, pellets, and mixed reactors), were applied to describe interaction over several orders of length scales (Schmitz and Tsotsis, 1983; Chang, 1983). Such presentation follows the pioneering work of Turing (1952), and has been extensively employed to study interaction of coupled reactors and particles. A proper discrete simulation of a distributed system requires a large number of cells, since experience showed that a small number usually leads to qualitative results that are dependent on the system size.

Catalytic Wires and Ribbons

Uncontrolled systems: moving and stationary fronts in bistable systems

Theory. Fronts may be sustained in a single-variable reaction-diffusion (or conduction) one-dimensional system, like wires or ribbons, that catalyzes a reaction with bistable kinetics. The source of multiplicity may be thermal acceleration in nonisothermal systems, reactant inhibition in an isothermal continuous porous layer, or even isothermal multiplicity in a surface that is free of any resistances. Single-variable systems that are generally described by

$$\tau_u u_t - L_u^2 u_{zz} = f(u;\alpha) \tag{11}$$

admit a moving front solution, in an infinitely long system, that connects the two stable solutions (u_+, u_-) of the source function (Figure 1I). Analytical solutions for front velocity (Mikhailov, 1991) are available only in a few cases: When the source function is cubic $f(u) = (u_- - u)(u - u_i)(u - u_+)$ the front velocity and profile are

$$c = \frac{L_u}{\sqrt{2}\,\tau_u}(u_+ + u_- - 2u_i),$$

$$u(z) = \frac{u_+ + u_-}{2} + \frac{(u_+ - u_-)}{2} tgh(z/\sqrt{2}L_u). \tag{12}$$

Hysteretic $f(u,\alpha)$ functions can sometimes be approximated

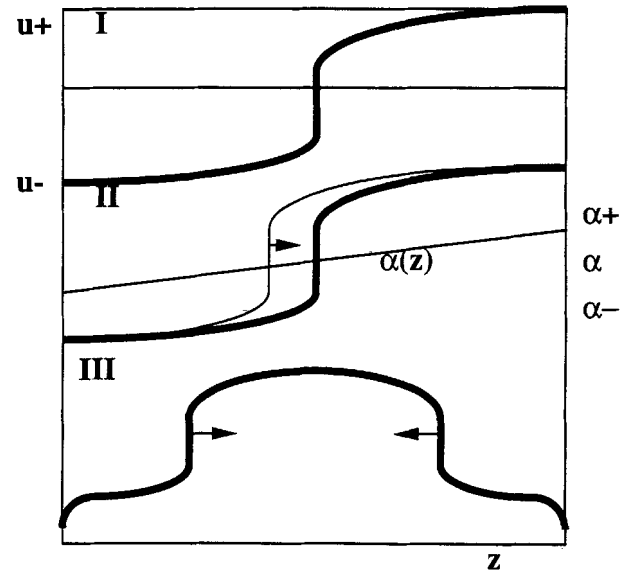

Figure 1. Characteristic front profiles that emerge on a catalytic wire.

With fixed activity and no-flux boundary conditions (I), on a wire with varying activity (α) (II), and on a wire with heat-loss at its edges (III). Stationary fronts are structurally unstable in case (I), but are stable in case (II), when activity and thermal profiles are of similar inclination.

by a piecewise linear form using a Heaviside function [$H(u) = 0$ for $u < 0$, $H(u) = 1$ for $u > 0$]. The function and front velocity then are (Mikhailov, 1991)

$$f(u,a) = -u + u_- + (u_+ + u_-)H(u - u_i);$$

$$c = \frac{L_u}{\tau_u}\frac{u_+ + u_- - 2u_i}{\sqrt{(u_i - u_-)(u_+ - u_i)}}. \tag{13}$$

In the general case, in an infinitely long system, the front reaches a constant shape and speed and the problem can be cast in the frame of a moving coordinate, $\chi = z/L_u - ct/\tau_u$. Finding the velocity corresponds to the eigenvalue problem of finding the heteroclinic trajectory of the system

$$u_\chi = p$$

$$p_\chi = -cu_\chi - f(u) \tag{14}$$

that connects the two saddle points $(u_-, 0)$ and $(u_+, 0)$. The front is stationary when

$$\int_{u_-(\alpha_0)}^{u_+(\alpha_0)} f(u;\,\alpha_0) = 0, \tag{15}$$

where α is a certain (say, kinetic) parameter and (u_-, u_+) are the two stable solutions of $f(u, \alpha_0) = 0$. Thus, stationary fronts are structurally unstable in one-variable systems, and their locus in the parameter space separates domains with an expanding upper or lower state. An approximate solution for the front velocity was suggested by Sheintuch (1990b) in the form

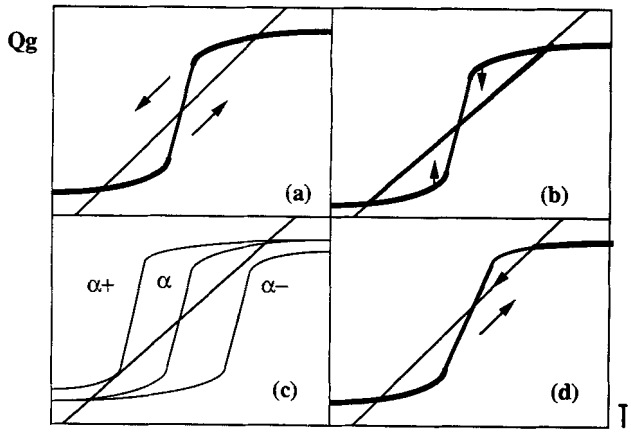

Figure 2. Intersection of heat-generation and heat-removal curves for a positive-order exothermic reaction and the corresponding stable (bold lines) branches.

In an uncontrolled (a) or controlled (b) uniformly active wire or in a wire with varying activity (c), or when heat loss at the edge is significant (d).

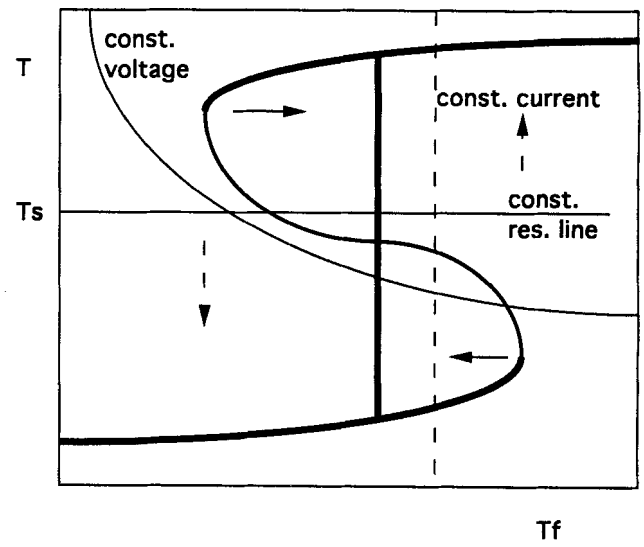

Figure 3. Bifurcation showing the dependence of average catalyst temperature on the equivalent fluid-temperature (which accounts for resistive heating) and the corresponding stable branches in a wire subject to one of three modes of control.

Constant current yields the regular hysteresis curve, while constant resistance or constant voltage control may stabilize a stationary front (vertical line).

$$\frac{U_f}{24}\left[\sqrt{U_f^2-4f_u(u_-)}+\sqrt{U_f^2-4f_u(u_+)}\right] = \frac{1}{(u_+-u_-)^2}\int_{u_-}^{u_+} f(u)\,du \quad (16)$$

with $U_f = c\tau_u/L_u$.

The steady-state solution of an exothermic reaction is commonly presented as the intersection of the heat-generation $Q_g = (-\Delta H)r$ and the heat removal lines $Q_r = h(T - T_f)a_V$ (Figure 2a). Stationary solutions in a uniform long catalyst exist only for a certain set of parameters for which the areas bounded by these two lines are equal (when Eq. 15 is satisfied with $f = Q_g - Q_r$; see Pismen, 1980). To find the conditions (T_f) that correspond to a stationary front, we adjust the ambient temperature, by displacing the heat removal line parallel to itself, to satisfy Eq. 15. In general, however, either the ignited (upper) or extinguished (lower) state will be more stable (Figure 2a) and the system will eventually achieve homogeneity. Varying a parameter (say T_f) will then result in a simple hysteresis curve (Figure 3, bold line) bound by the limit points of ignition and extinction.

Observations. Barelko et al. (1978) measured the front velocity, separating the ignited and extinguished state of a resistively heated (with a constant current) Pt wire catalyzing ammonia oxidation, by recording the wire resistance and by photographing the glowing wire. For a sufficiently low or high current the extinguished or ignited zone expanded, as expected from theory. But, contrary to the prediction of the single-variable model, Barelko et al. found an intermediate domain where structurally stable stationary fronts exist: that is, the front could be placed at will at almost any position (Figure 4a). Recently, Philippou et al. (1993) reproduced this experiment on a Pt ribbon using resistance measurements and IR thermography for monitoring the thermal profile (Figure 4b). They showed that in the intermediate regime the front was not stationary, but moved at a considerably smaller velocity. These observations suggest that a single-variable reaction-diffusion model cannot account for these results, as it lacks a mechanism for arresting or slowing the front.

Nonuniform Systems. We consider below the effect of space-dependent parameters (e.g., catalytic activity) and of boundary conditions of the Neuman form. We show first that a nonuniformity in parameters can create structurally stable stationary fronts. (We use the term "nonuniformity" of parameters to distinguish it from inhomogeneity of the solution; by almost homogeneous solutions we imply that the whole system is at a state that belongs to the same, upper or lower, branch.) Suppose that parameter α in Eq. 11 is space dependent, $\alpha = \alpha(z)$, but monotonic, and that a stationary front exists for certain α_0, which is within the range spanned by $\alpha(z)$ and it occurs at a certain z_0 (Figure 1, curve II). Now, we can place the front at z_0 so that the parameter (α) and the variable (u) profiles show a similar (curve II) or opposite inclination (not shown). In the latter case, if the front is perturbed to a new position with $\alpha > \alpha_0$ the upper state is more stable and it will expand until the front moves out of the system. In the former case, however, the front will move back toward its stationary position and the front is stable (Figure 1, curve II). If we change the operating condition now (say, T_f or C_f) and try to obtain a bifurcation diagram, we find that the front will move to a new position where the activity satisfies the stationarity condition. Analysis of such a system shows that the wider the domain of nonuniformity, the larger the domain over which stationary fronts exist. To show that, let us denote the Q_g curves of the largest and the smallest activity with α_+ and α_- (Figure 2c). Obviously, an ignited or extinguished state cannot exist unless $ha_V(T - T_f)$ intersects the upper (lower) branch of all $Q_g(T, a)$ curves with $\alpha \in$

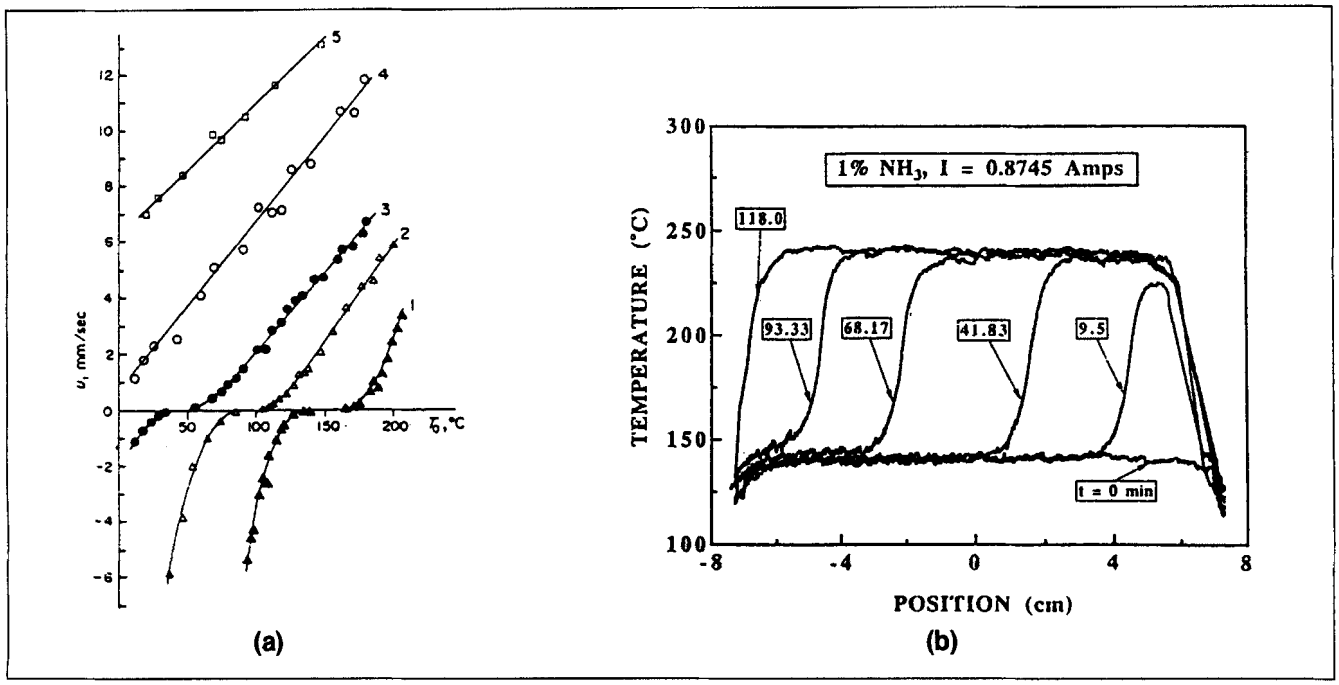

Figure 4. Thermal front propagation on a Pt catalytic wire or ribbon during ammonia oxidation.

(a) Front velocity dependence on ambient temperature and reactant concentration (1% (line 1), 2% (2), 3% (3), 5% (4), and 8% (5) ammonia; after Barelko et al., 1978). (b) Transient temperature profiles observed with 1% ammonia using IR thermography. Reproduced with permission from Philippou et al. (1993).

(α_-, α_+). When that is not possible (as in Figure 2c), a stationary front must be established.

The preceding analysis was limited to zero flux boundary conditions. In an actual catalytic wire, which is connected to two inactive ports at its edges, the boundary conditions should account for some heat loss through the ports. With high heat loss the edge temperature should approach the ambient one. Suppose now that the activity is uniform but the edge conditions specify that $T = T_-$. If the system lies at an ignited state, outside the domain of steady-state multiplicity, the edge effect will be limited to a narrow transition zone. In the domain where the ignited state is more stable, the front connecting T_- and T_+ cannot propagate inward, and again will lie close to the edge. However, when the lower steady state is more stable, this front will conquer the whole surface (Figure 1, curve III); thus, under these conditions an ignited homogeneous state cannot be sustained, while it can be sustained in a wire with no-flux boundary conditions. The resulting bifurcation diagram is shown in Figure 2d. Similar results are expected when the edge temperature lies even below T_-.

Uncontrolled systems: excitable and oscillatory (two-variable)

Theory. The emergence of patterns in catalytic reactions is surprising since, as discussed earlier, our current understanding suggests that catalytic oscillators are governed by the interaction of a fast and long-range activator (the catalyst temperature) with a slow and localized inhibitor (Sheintuch and Pismen, 1981). That is contrary to most mathematical models of reaction-diffusion systems that, following Turing's classic analysis, predict pattern formation with a short-range activator and a long-range inhibitor. The length scale of inhibitor is set to be larger than that of activator by assigning it either higher diffusivity, a lower pseudo-first-order rate constant, or both. An inhibitor, with a sufficiently long length scale, senses changes in the front position and may counteract and arrest its motion. Such a mechanism can account for the front behavior observed during ammonia oxidation. The same mechanism induces pattern formation in an *endothermic* reaction of autoinhibitory (e.g., Langmuir–Hinshelwood) kinetics catalyzed by a wire or a ribbon (Hefer and Sheintuch, 1986; Sheintuch and Hefer, 1988). This problem is described then by a two-variable one-dimensional model and reactant concentration is the short-ranged autocatalytic variable, while the long-ranged catalyst temperature is the inhibitor. In most high-pressure *exothermic* catalytic systems, however, the catalyst temperature is the activator (u) and its length scale is larger than that of the inhibitor (v), which is believed to be a slowly changing surface concentration. Such systems are typically of the form

$$\begin{cases} u_t - u_{zz} = f(u,v) \\ 1/\epsilon\, v_t = g(u,v), \end{cases} \tag{17}$$

where $\epsilon = \tau_u/\tau_v$, the ratio of time scales, is usually a small parameter and $f(u,v) = 0$ is a multivalued curve. The relative disposition of the nullcurves is usually classified as excitable, when the steady state is locally stable but excitable (Figure 5a), as oscillatory, when the steady state is unstable (Figure 5b), and as bistable (Figure 5c). The system may admit a traveling pulse solution or homogeneous oscillations, in a uniform one-dimensional medium, and is unlikely to exhibit sustained spatiotemporal patterns. Patterns may emerge due to

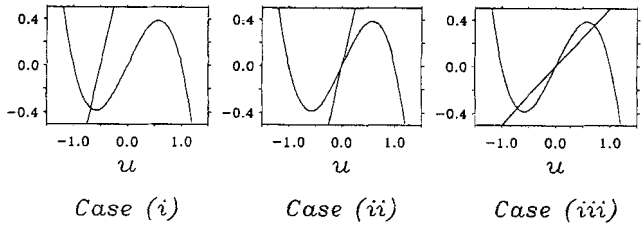

Figure 5. Three basic cases of dynamic behavior differing in their phase plane nature.

Excitable (i), oscillatory (ii), and bistable (iii) kinetics. Courtesy of Meron (1992).

global effects, as explained below; to understand these motions we need to review the properties of such excitable or oscillatory systems.

Excitable media are extended nonequilibrium systems having homogeneous rest states that are linearly stable but susceptible to finite perturbations. A variety of wave patterns can be triggered including solitary waves in one dimension, target patterns or spiral waves in the plane, and expanding roll waves or rotating scroll waves in the space. Solitary waves propagate at constant speed and shape but, unlike solitons, annihilate each other in face-to-face collision. Excitable media also support continuous families of periodic wavetrains when the system is triggered continuously. Two basic theoretical approaches have been applied to analyze such motions: A singular perturbation approach makes a distinction between outer (excited and recovery) regions and inner front regions (Meron, 1992), while kinematic theories review solitary waves as integral entities. The former approach exploits the smallness of ϵ, while the latter assumes long-wave patterns. Excitable waves have been observed and studied in the BZ reaction, the axon of a nerve cell, cardiac tissues, and the corresponding models like the FKN mechanism and the FitzHugh-Nagumo model (Mikhailov, 1991).

We now present the main results of the singular perturbation approach (Meron, 1992). Triggering the edge of an excitable system will send a front traveling at constant speed. After a certain period the perturbed position will relax, undergo an opposite transition, and will send a second front in the direction of the leading one. Eventually, the two fronts will form a pulse, traveling at a constant speed and shape. For small ϵ the pulse consists of a wavefront and waveback that separate the domain into three zones (Figure 6a): the rest state, to the left of the leading front, the excited state, between the fronts, and the refractory tail. At the front position the autocatalytic variable (u) undergoes a sharp jump, while the other (v) variable changes slowly and, to a first approximation, its spatial gradient is negligible. In the limit of $\epsilon \to 0$, changes in activity are slow compared with front motion and the solution is derived by matching the outer and inner solutions. In the outer region, u varies smoothly in space and in time, while in the inner, wave-front or -back, region u changes abruptly. In the outer region, u follows adiabatically

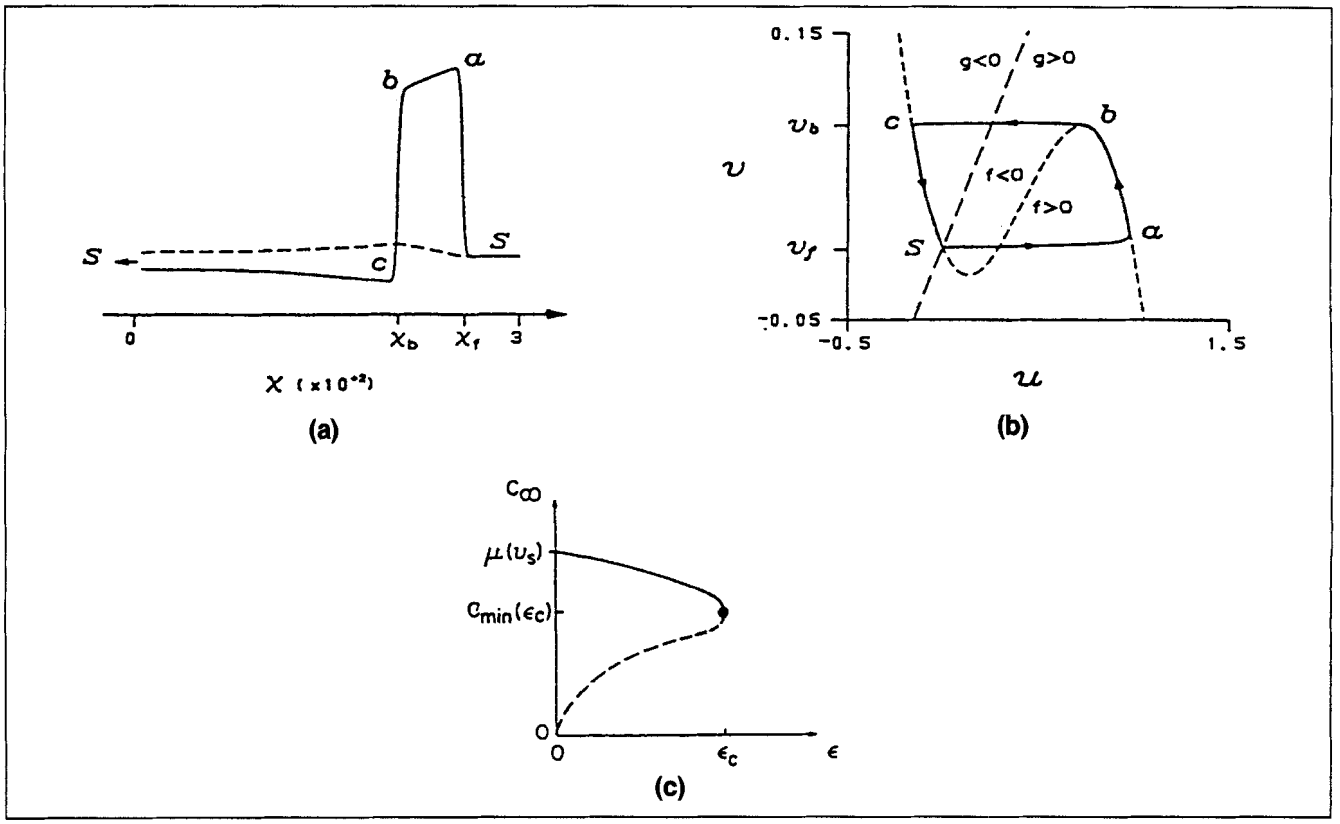

Figure 6. Properties of solitary waves in an excitable medium.

(a) Profiles of the activator ($u(\chi)$, $\chi = z - ct$, solid line) and inhibitor ($v(\chi)$, broken line). (b) Phase portrait of the solitary wave solution (homoclinic orbit). (c) Propagation speed dependence on time scale separation (ϵ). Solitary waves cannot be sustained above ϵ_c. Reproduced with permission from Meron (1992).

the slow changes in v. The spatial and temporal derivatives of u are small and, to the zeroth order of ϵ, the activator balance becomes an algebraic equation $f(u,v)=0$, which can be solved for u (Figure 6b). The upper and lower stable solution branches of this equation are denoted by $u_-(v)$ and $u_+(v)$. Since we are looking for the solution in the form of a solitary wave that propagates at the velocity c_∞ through the medium that is initially at rest at $v=v_s$, we have for the outer solution:

$$
\begin{aligned}
&u=u_-(v), \quad c_\infty v' + \epsilon G_-(v)=0, \quad -\infty<\chi<\chi_b\\
&u=u_+(v), \quad c_\infty v' + \epsilon G_+(v)=0, \quad \chi_b<\chi<\chi_f\\
&u=u_-(v)=u_-(v_s), \quad c_\infty v' + \epsilon G_-(v)=0, \quad \chi_f<\chi<\infty\\
&\chi=z-c_\infty t, \quad G_\pm(v)=g[u_\pm(v),v],
\end{aligned}
\tag{18}
$$

where χ_b and χ_f denote the pulse-front and -back position (Figure 6a) and $v'=\partial v/\partial\chi$. The inhibitor (or controller) solution must be continuously differentiable at the fronts, which yields the following boundary conditions:

$$
\begin{aligned}
&v(\chi\to\chi_b^+)=v(\chi\to\chi_b^-)=v_b, \quad v'(\chi\to\chi_b^+)=v'(\chi\to\chi_b^-)\\
&v(\chi\to\chi_f^-)=v(-\infty)=v_s \quad v'(\chi\to\chi_f^-)=v'(\chi\to-\infty).
\end{aligned}
\tag{19}
$$

The solution of Eqs. 18–19 provides the large length scale structure of the pulse. To find the inner solution, the inhibitor value is assumed constant at the front position, which yields the following system of equations

$$
\begin{aligned}
&(a)\quad u_f'' + c_\infty u_f' + f(u_f,v_s)=0\\
&(b)\quad u_b'' + c_\infty u_b' + f(u_b,v_b)=0\\
&u_f(\chi-\chi_f)=\begin{cases} u_-(v_s) & \chi\to\infty\\ u_+(v_s) & \chi\to-\infty\end{cases}\\
&u_b(\chi-\chi_b)=\begin{cases} u_+(v_b) & \chi\to\infty\\ u_-(v_b) & \chi\to-\infty\end{cases}.
\end{aligned}
\tag{20}
$$

The leading front travels in a domain with $v=v_s$ and its velocity can be determined or approximated from the velocity of a single variable system. In order for the pulse to preserve its shape, the waveback velocity should match that of the wavefront velocity. This determines v_f at the waveback. Since c_∞ is usually a monotone decreasing function of v, with a stationary velocity at $v=v^*$ determined by

$$
\int_{u_-(v^*)}^{u_+(v^*)} f(u,v^*)\,du=0, \tag{21}
$$

it is evident that v_b and v_f lie at opposite sides of v^*. If the largest back front velocity cannot match c_∞, than the back transition is determined by local dynamics and the back wave is called a *phase-wave*.

When time-scale separation is not wide, the outer and inner solution construction is no longer valid. Rewriting Eq. 17 in the moving frame coordinates, we find

$$
\begin{cases} u'' + c_\infty u' + f(u,v)=0\\ c_\infty v' + \epsilon g(u,v)=0. \end{cases}
\tag{22}
$$

Expanding u, v, and c_∞ in powers of ϵ,

$$
\begin{aligned}
&u=u_f+\epsilon u_1+\ldots \qquad v=v_f+\epsilon v_1+\ldots\\
&c=\mu(v_s)+\epsilon c_1+\ldots.
\end{aligned}
\tag{23}
$$

As expected, the zero-order solution was shown to be $c=c_\infty=\mu(v_s)$ (Meron, 1992), while the first-order correction is given by

$$
c_1=\frac{\int_{-\infty}^{\infty} d\chi\,\xi^+ v_1\partial_v f(u,v)|_{u_f,v_s}}{\int_{-\infty}^{\infty} d\chi\,\xi^+\xi};
$$

$$
v_1(\chi,v_s)=\frac{1}{\mu(v_s)}\int_\chi^\infty d\chi'\,g(u_f(\chi'),v_s),
\tag{24}
$$

where $\xi=u_f'$, $\xi^+=u_f'\exp(\mu(v_s)\chi)$. Generally c_1 is a negative quantity, which implies that the excitable wave velocity declines as ϵ increases. At certain ϵ_c the velocity reaches a limit point that connects the stable high-amplitude solitary wave, described earlier, with low-amplitude unstable pulse solutions (Figure 6c; Meron, 1992). Beyond that critical ϵ_c an excitable wave cannot be sustained.

A continuous periodic triggering of an excitable medium yields a traveling wave solution. Target and spiral-wave patterns are two-dimensional realizations of these solutions. Wave trains are usually characterized by dispersion relations that describe the relation between the speed of propagation and the traveling-wave period. The repeated structure consists of a wavefront (at χ_f, with a corresponding v_f), an excited region, a waveback and a refractory region that continues till the next front. The two fronts travel at the same velocity, that is, $c=\mu(v_f)=-\mu(v_b)$. Specifying the wave train velocity determines the corresponding v_f and v_b. The two domains separating the fronts are of the following sizes:

$$
\begin{aligned}
&\lambda_+(v_f)=\chi_f-\chi_b=\mu(v_f)T_+(v_f); \qquad \epsilon T_+=\int_{v_f}^{v_b}\frac{dv}{G_+(v)}\\
&\lambda_-(v_f)=\chi_b-\chi_s=-\mu(v_f)T_-(v_f); \qquad \epsilon T_-=\int_{v_f}^{v_b}\frac{dv}{G_-(v)}
\end{aligned}
\tag{25}
$$

and are readily computed. Dispersion relations typically show a limit point separating the high-speed stable solutions from the low-speed unstable solutions.

While a pulse on a wire eventually travels out of the system, it may be sustained on a *ring* with v_f and v_b that yield fronts of equal velocity and with a ring perimeter that matches the wave period ($\lambda_+ + \lambda_-$, Eq. 25) or its multiple. The small-

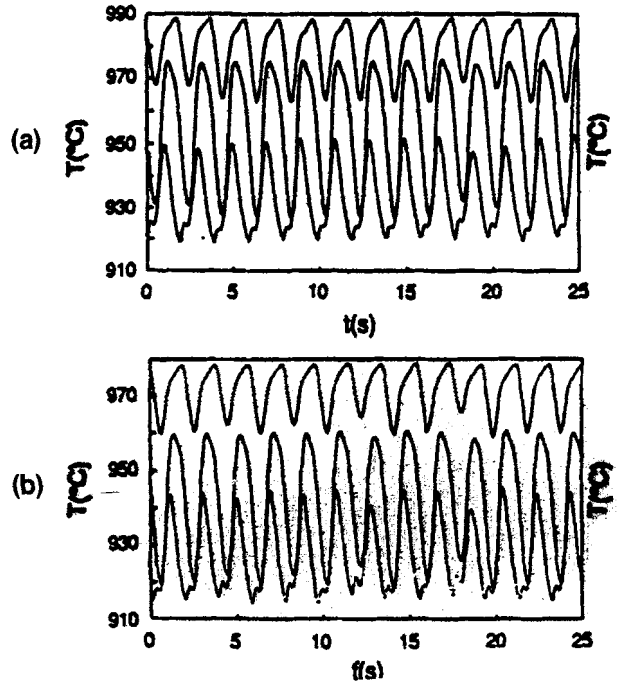

Figure 7. Temporal traces of temperature oscillations observed at three points on a Pt wire catalyzing ammonia oxidation with 28% ammonia in air at 800°C.

(a) Shortly after startup. (b) After 7 h; the three points are approximately 0.8 cm apart. Reproduced with permission from Cordonier and Schmidt (1989).

est ring that can harbor a moving pulse is the limiting value of the dispersion relation, a certain $L_{\min}(\epsilon)$. We return to this problem in the sixth section.

Wave trains on a wire and a rotating pulse on a ring may be sustained even with oscillatory kinetics (i.e., when the homogeneous state is unstable, also termed Hopf–Turing systems), but they will require special initial conditions for their inception. Homogeneous initial conditions will typically yield a homogeneous oscillatory solution.

Excitable pulses annihilate each other upon oscillation because of the refractory zone behind the waveback. The introduction of defects, however, with parameters that differ from those of the rest of the surface can lead to soliton-like behavior: that is, pulses may collide and reflect from each other (Bar et al., 1992).

Observations. Excitable waves, triggered by a perturbation of a catalytic wire or ribbon at steady state, were not studied under high-pressure conditions. Several observations of sustained patterns in catalytic wires have been reported, but their identification in terms of a qualitative model is still ambiguous. The first evidence of a regular pattern in catalytic systems, in the form of two temperature pulses emanating from a source point and traveling in opposite directions, was presented by Cordonier and Schmidt (1989) during ammonia oxidation on a Pt wire heated by a constant current. The system was monitored with the array of 6 IR-sensitive photodiods. Spatial nonuniformity is evident in Figure 7, but so is the phase difference between the three traces. Waves of different waveforms and velocities in the range 0–5 cm/s were reported. Spatiotemporal complexity was shown to be induced by the formation of the two pacemakers. No topographical differences of the area around the pacemaker could be detected with scanning electron microscopy (SEM), but the active center position was fixed over a series of experiments. The second center emerged with changing flow rate. The authors explained the observed wave propagation in terms of a surface reaction-diffusion model with oscillatory boundary conditions (a pacemaker) imposed at the boundaries.

Antiphase oscillations were observed by Cordonier et al. (1989), using a photodiode array, during the endothermic decomposition of methylamine catalyzed by a 5-cm-long Rh wire (Figure 8). The wire can be roughly described by two sections that oscillate out of phase; the boundary between the two sections moved slowly and was associated with a slow deactivation process. Local temperature oscillations were periodic. In a similar study with a Pt wire all measured points were oscillating synchronously with no measurable time lag. With an Ir wire, however, the temporal pattern was chaotic, but again all the points on the wire were oscillating in phase. No theoretical explanation of the phenomena was attempted.

Philippou and Luss (1992) in their study of propylene oxidation on a 14.5-cm-long Pt ribbon heated by constant electrical current, using IR thermography, observed aperiodic birth of fronts near the support and their propagation inside the ribbon. The front stopped at a certain position and moved backward before another front originated at the other support.

Before spatially resolving experiments were designed, the spatially nonuniform character of catalyst performance could be inferred from comparison of integral reactor characteristics, such as reactant conversion or overall heat-generation function, with measurements of local temperature. Tsai et al. (1988) observed that temporal thermal oscillations of two halves of a Pt ring, during CO oxidation, was simpler than that of the whole ring.

Controlled wires: bistable media

Theory. While stable stationary fronts are not possible in a one-variable system with constant coefficients, they do exist in systems subject to global interaction, in which every point interacts will all other points through a common pool. The simplest example of global interaction is due to control of a space-averaged property. The thermochemic method, in which the wire resistance (i.e., temperature) or voltage is kept constant by applying resistive heating, has been widely applied in studies of catalytic kinetics and dynamics over metal wires in order to keep the system isothermal. Analysis of such control (Sheintuch and Schmidt, 1986) showed, however, that it cannot stabilize a thermally unstable state in a sufficiently long systems (few L_T, typically few mm). Instead, the wire prefers to attain an inhomogeneous solution with a stable front separating the ignited and extinguished states. The effect of resistive heating amounts mainly to increasing the effective ambient temperature (T_f): $Q_r = ha_V(T - T_f) = ha_V(T - T_a) - I^2R$, where T_a is the actual ambient temperature (see Sheintuch and Schmidt, 1986; and Sheintuch, 1989b, for a detailed analysis). A catalytic wire or ribbon is described by a single-variable enthalpy balance with unspecified T_f, but subject to the control setpoint that $\langle T \rangle = T_s$. (T_f can be determined by integrating the enthalpy balance to yield $T_f = T_s -$

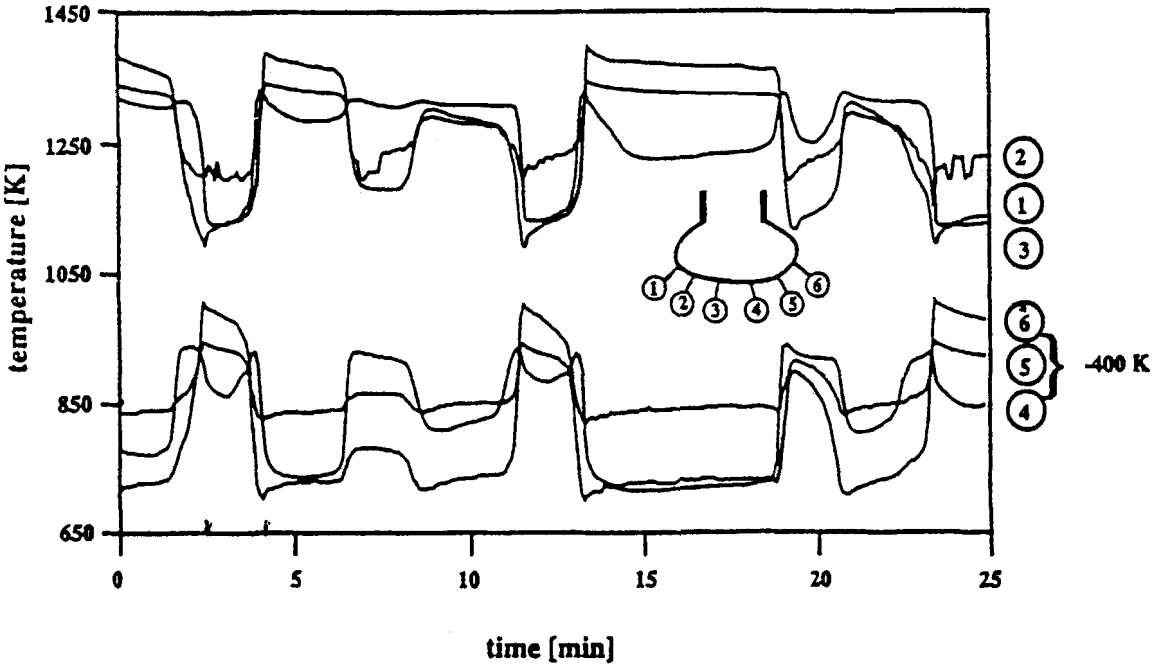

Figure 8. Antiphase temperature oscillations during methylamine decomposition on a Rh wire.
Reproduced with permission from Cordonier et al., (1989).

$(\Delta h)\langle r(T)\rangle/ha_V$.) The solution in a long system takes the form of a stationary front, at a position that satisfies the setpoint, and with a control variable (T_f) that satisfies the stationarity condition of the front: The front is stable since the expansion of the ignited zone will result in declining resistive current that will render the ignited state less stable and move the front into its stationary positions. The graphical construction of zero velocity condition is shown in Figure 2b; Eq. 15 implies equality of the areas bound by $Q_g(T)$ and $ha_V(T - T_f)$. The stable branches are denoted by bold lines, showing domains of coexistence of inhomogeneous solutions with the ignited or extinguished homogeneous state. (The diagram may change when heat loss through the edges is accounted for: see Sheintuch and Schmidt, 1986.) The resulting bifurcation diagram with varying T_s is shown in Figure 3. In the constant-resistance mode we vary T (the ordinate in Figure 3) by changing the setpoint. Changing current in the constant-current mode amounts to shifting T_f (the abscissa), resulting in simple hysteresis. In the constant-voltage case $T_f = T_a + V^2/R(T)ha_v$ and, since the resistance is linear with the temperature $[R = R_0 + R_1(T - T_1)]$, the steady state is the intersection of an enthalpy balance with a hyperbolic operating line. The constant-voltage line may intersect the enthalpy line at three stable (two homogeneous and one asymmetric) branches and tristability may be realized.

Observations. The existence of stationary fronts in a catalytic wire maintained at a preset average temperature was verified by Lobban et al. (1989) during ammonia oxidation on a Pt ribbon. They were able to obtain multiplicity of a stationary front solution with an almost homogeneous states (edge effects due to heat loss were evident) under the same resistance setpoint (Figure 9a). The fronts observed in this study were sharp, typically 0.5 cm in width—a value that agrees with the characteristic thermal diffusion length. Similar patterns were obtained under constant-voltage control by Phillipou and Luss (1993). In the latter case, they were able to obtain two (almost mirror-imaged) stationary front solutions under the same operating conditions (Figure 9b).

Stationary fronts have been inferred to exist on a Pt wire catalyzing ammonia, ethylene, propylene and isobutylene oxidation (Sheintuch and Schmidt, 1986); this conclusion was based on the observation that the measured heat-generation rate increases with the set temperature like $h(T_s - T_f^*)$, as expected from theory (T_f^* is the value that sustains a stationary front).

Controlled wires: oscillatory systems

Observations. Phillipou et al. (1991) observed temperature pulses moving back and forth, during propylene oxidation on a 14.5-cm-long Pt ribbon heated resistively to maintain a preset resistance (Figure 10; α, β, γ denote three successive snapshots). They used hot wire anemometry to follow the overall heat generation of the exothermic reaction and IR thermography to measure the temperature profile over the ribbon. The pulse did not travel through a section of the wire, probably due to its low activity, and expanded and contracted during its motion over the other section. The space-averaged reaction rate oscillated at a higher frequency than that of local temperatures. Analysis of heat-generation time series revealed quasi-periodic oscillations when a single pulse motion was observed locally and inception of a second pulse was documented as a route to chaotic dynamics. These observations were the incentive for the theoretical studies discussed below. Under constant voltage conditions this reaction also exhibited moving fronts that originated at one edge and propagated toward the other support (Phillipou and Luss, 1993). The front stopped at a certain intermediate position

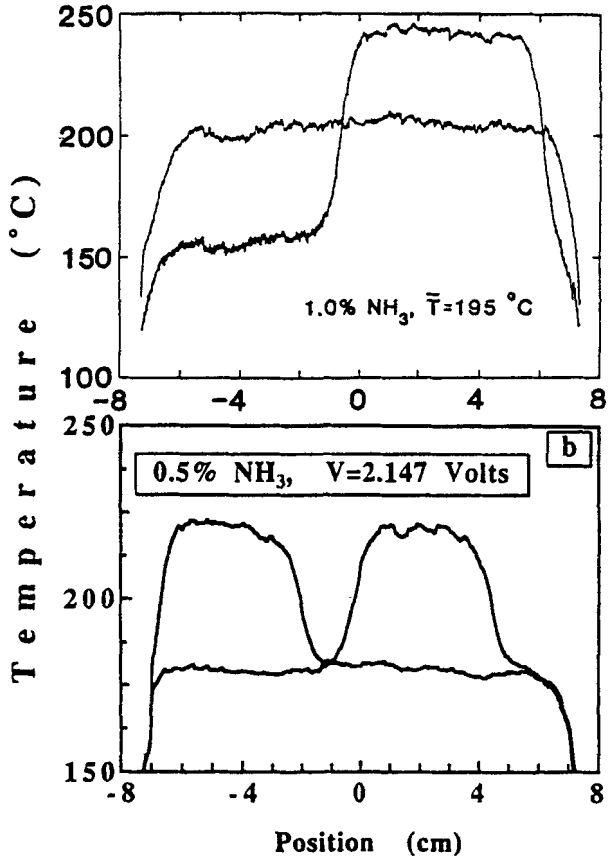

Figure 9. Inhomogeneous solutions observed during ammonia oxidation on a controlled Pt ribbon.

(a) Two temperature profiles observed in the constant resistance mode. (After Lobban and Luss, 1989; reproduced with permission of the authors.) (b) Two mirror-imaged solutions under constant voltage control. Reproduced with permission from authors Philippou and Luss (1993).

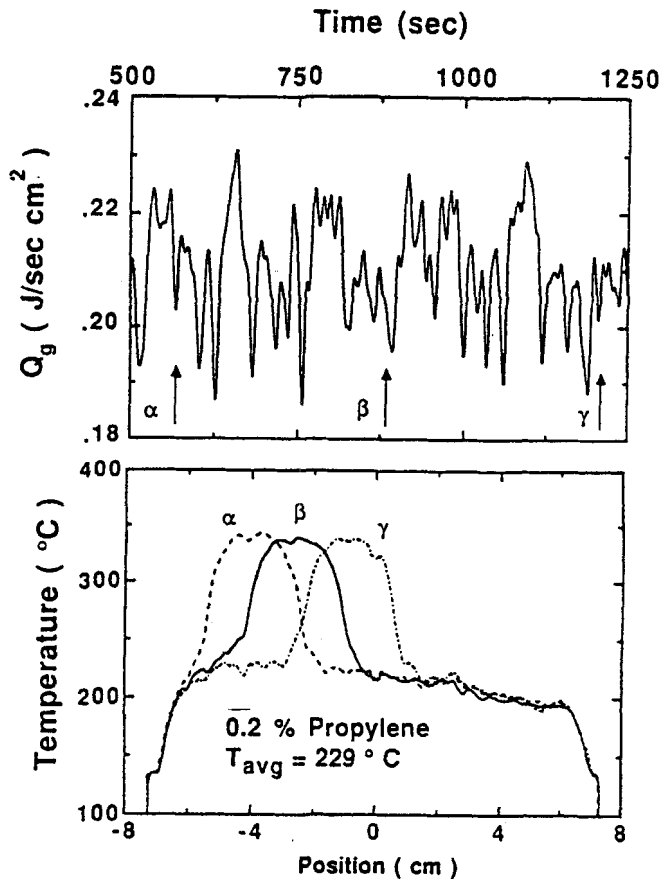

Figure 10. Back-and-forth pulse motion during propylene oxidation on a controlled Pt wire at an average temperature of 229°C.

(a) Time trace of the average heat generation. (b) Three spatial snapshots. Reproduced with permission from Phillippou et al. (1991).

and moved backward before another front originated at the other support. In both constant-voltage and constant-resistance experiments the front velocity was ~ 0.1 cm/s.

Modeling. As was already stated, stationary fronts may be formed when a chemical reaction, with bistable kinetics, is carried out on a catalytic ribbon, the average spatial temperature of which is kept constant by a controller. Similarly, spatiotemporal temperature patterns are formed when an oscillatory reaction is subject to constant-temperature control. We consider a catalytic ribbon, placed in a fluid stream of constant temperature and reactant composition, on which an exothermic chemical reaction occurs. The kinetic model incorporates surface temperature (T) and the local catalytic activity (θ^*) as its dynamic variables. The fast control adjusts the electrical current in the ribbon (the effective ambient temperature, T_f) so that its total resistance (average temperature) remains constant at a preset value (T_s); recall that T_f is linearly related to the average reaction rate $\langle r \rangle$.

Early analysis of this model (Sheintuch, 1989a) assumed that the reaction fronts are localized, either because of nonuniformities in the wire or due to slow front propagation. The wire is described then by several homogeneous oscillators subject to the control conditions. The two or more sections of the wire then oscillate out of phase in order to maintain the set average temperature. On the phase plane diagram the motion of the representative points is like "ponies on a merry-go-round" (Sheintuch, 1989a). Wide domains of aperiodic solutions emerge when three or more sections exist. Analysis of the continuous model (Middya et al., 1993a,b, 1994a,b) revealed, however, that heat conduction is an important mechanism of interaction along the ribbon, and it induces temperature fronts and pulses. The simulated patterns were classified into four major types: homogeneous, localized, moving, and mixed. Localized patterns incorporate fronts or pulses with stationary or oscillating front-positions. These include (Figure 11):

- Stationary and oscillatory fronts (Figure 11a,b)
- Breathing pulses that expand and contract
- Antiphase oscillations (Figure 11c).

Moving patterns include:

- Unidirectional pulses that are born at one edge, travel toward the other edge, and disappear while a new one is born at the original edge (Figure 11d)
- Source point from which two pulses emanate and move in opposite directions until their disappearance (Figure 11e); several source points may coexist
- Pulses that move back and forth (Figure 11f).

To gain some understanding of these motions let us follow

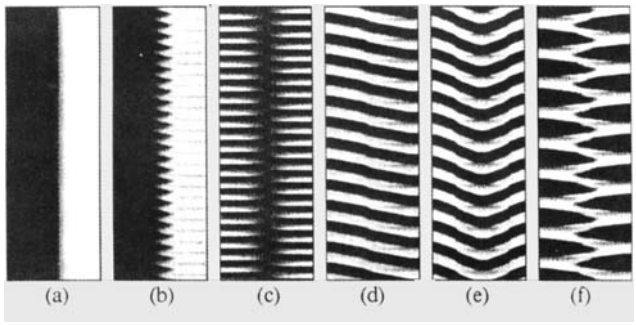

Figure 11. Spatiotemporal patterns simulated for controlled catalytic wires with oscillatory kinetics. Stationary (a) or oscillatory (b) fronts, antiphase oscillations (c), unidirectional pulse (d), source point (e) and back-and-forth pulses (f).

Patterns were computed with a cubic kinetic function (Middya et al., 1994b, but similar patterns were obtained for realistic models, Middya et al., 1993a). Patterns are presented in the time-space plane with gray and light shades corresponding to extinguished and ignited local states, respectively.

them on the (T, θ) phase plane. In antiphase oscillations the ribbon consists of two regions having temperature A and A' (Figure 12a), separated by a narrow zone. This disposition is synclinal (activity and temperature fronts have similar inclination; Pismen, 1980), the front is stationary, and the hot region deactivates and the cold region activates. Eventually, the hot section reaches extinction (point C in Figure 12a). This triggers the control and ignites the cold section (point C'). Consider now a unidirectional pulse (Figure 12b). If the leading and trailing fronts travel at the same velocity, the average temperature does not change before the leading front approaches the support. The ignition front occurs at $\theta_B > \theta_s^*$ (of the stationary front), while extinction occurs at $\theta_D < \theta_s^*$. In general, the two fronts move at the same average velocity, as the control changes the current to counteract any change in the average temperature or pulse width. When the ignited front reaches the support and disappears, the current starts to increase, raising the temperature of all points on the ribbon and slowing the movement of the extinction front DE. The highest activity of the ribbon is at the other support, and, as the current increases to some critical value, ignition occurs. Thus, as the old pulse propagates out of the ribbon, a new pulse is formed at the other support, grows, and then moves toward the second support.

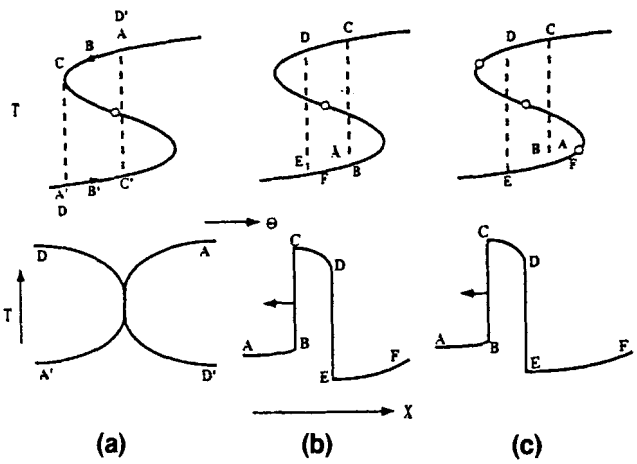

Figure 12. Spatial patterns and null curves of the main patterns that emerge in controlled wires.

See description in text; after Middya et al. (1993a). (a) Antiphase oscillation. (b) Unidirectional pulse. (c) Back-and-forth pulse.

When the system is bistable, a back-and-forth pulse may exist. The starting sequence of events is similar to the previous scenario. After the ignited front leaves the system at the support, the controller increases the current, slowing down the movement of the extinction front. In the wake of that front the activity is low and the pulse cannot turn around and become an ignition front. When multiple solutions exist, the pulse may approach a stationary-front solution. This gives the low-activity section enough time to recover. But this stationary anticlinal front is unstable for sufficiently small time scale separation, and it propagates as an ignition front in the opposite direction (Figure 12c), into a domain that has been activated by now. While these patterns have been identified by simple visual inspection, with cubic polynomial kinetics it is possible to define the various patterns by their symmetry properties (Middya et al., 1994b). The transitions between some of these patterns are intricate and proceed via a sequence of bifurcations that is still under study. The transition between back-and-forth and unidirectional pulses occurs through complex patterns that include mixed mode motions (Middya et al., 1993b).

Electrochemical systems

Antiphase oscillations of spatial current distribution during anodic dissolution of a nickel wire in sulfuric acid solution were observed in the galvanostatic mode of operation (Figure 13b; Lev et al., 1988, 1990). In this mode, the applied overall current remained constant, but the local current density varied. A set of microreference electrodes, situated close to the anodized nickel wire, was used to record the local activity. Pattern selection depended crucially on the control mode: traveling pulses were observed under almost-potentiostatic conditions. The latter conditions were obtained by incorporating a small ohmic resistance between the reference and working electrodes. Both the current and the true electrode potential oscillate during such an operation, since the potential and current become linearly dependent on Ohm's law.

The model constructed to simulate these behaviors and to demonstrate the relation between the pattern established and the applied control accounts for the surface potential, for the solution potential through which communication occurs, and for the degree of surface activity, which changes slowly and does not diffuse (Haim et al., 1992). The model accounts for spatial potential distribution in the directions parallel and perpendicular to the wire. The potential difference between the electrodes is space-independent, but the potential of the electrolyte solution and the electric double layer close to the anode is space-dependent. The model simulated the antiphase oscillations observed under galvanostatic conditions (Figure 13a), and the traveling waves observed when a small external resistor was incorporated in the circuit. The simulations demonstrated the change in pattern as the external resistor (R) was varied.

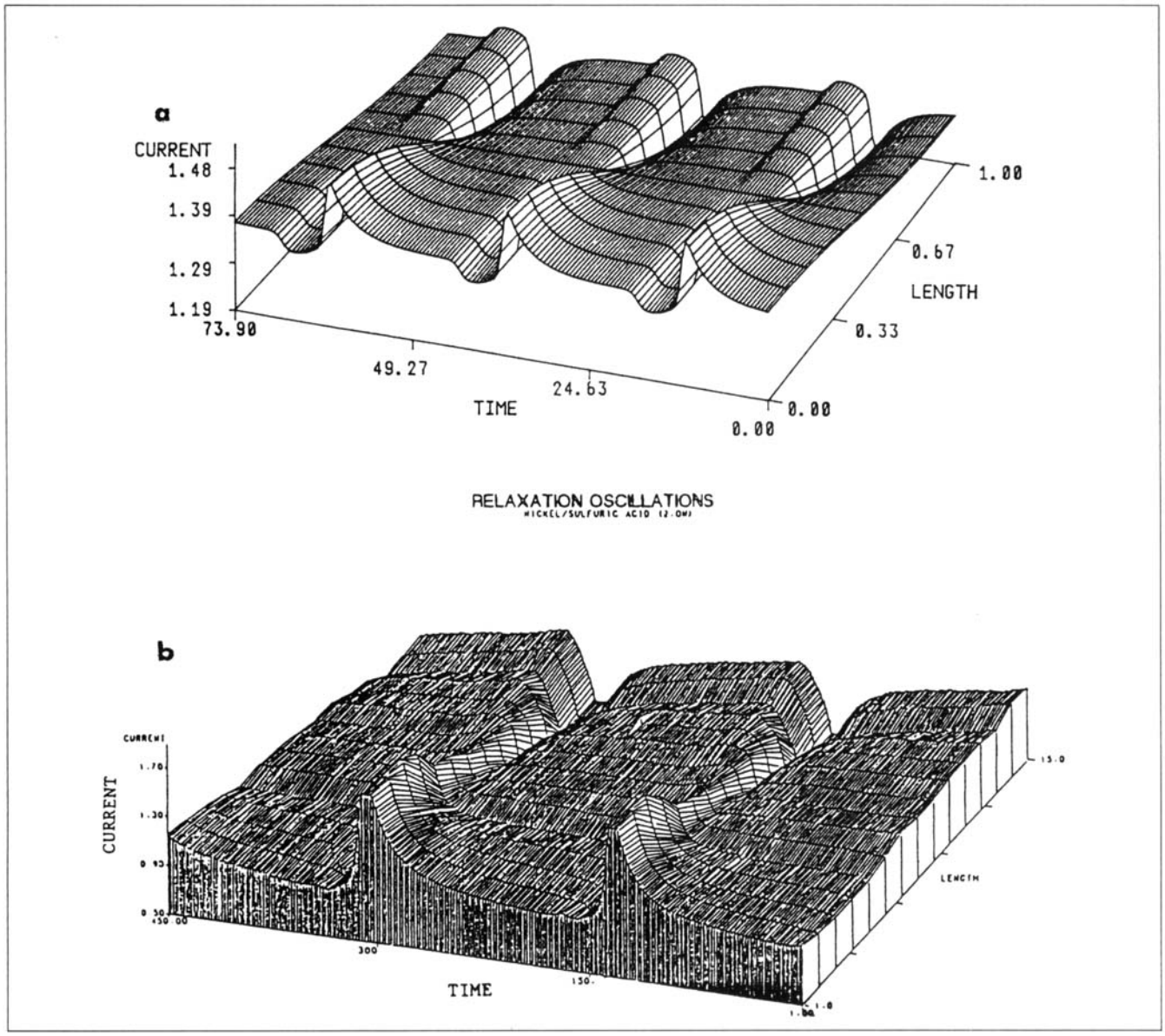

Figure 13. Antiphase current oscillations simulated (a) and observed (b) for anodic Ni wire dissolution operating in the constant current model.

From Haim et al. (1992).

Catalytic Disks and Wafers

Theory. Typical reaction-diffusion patterns on a plane of excitable medium are target patterns and spiral waves. The analysis is similar to that of pulses on a wire except that front curvature has a significant effect on its velocity. Positive curvature (where the center of curvature is behind the front) reduces the speed of propagation, since the convex geometry reduces the diffusion flux into the resting medium. Negative curvatures increase the front velocity. For small curvatures (κ), the curvature-speed relation is

$$c_r = c - D_u \kappa, \tag{26}$$

where c_r is the normal velocity, c is the velocity of a linear front, and D_u is the activator diffusivity (Mikhailov, 1991). While there is an extensive theory on this subject, we do not review it here, as it does not account for most observations of high-pressure patterns.

Observations. Most patterns observed on two-dimensional catalytic systems did not conform with any known motion of reaction-diffusion systems. Investigators usually attribute the ambiguity to nonuniformity of surface properties. Several studies demonstrated the existence of one or more pacing centers that determine the motion of the whole surface. In several cases aperiodic solutions were shown to be associated with the interaction between two or more such pacing centers. Considerable progress in elucidating and analyzing spatiotemporal temperature patterns was made with the employment of IR thermography, permitting 0.1-mm resolution at the surface. Yet, the very first application of this method (Brown et al., 1985) showed significant temperature differ-

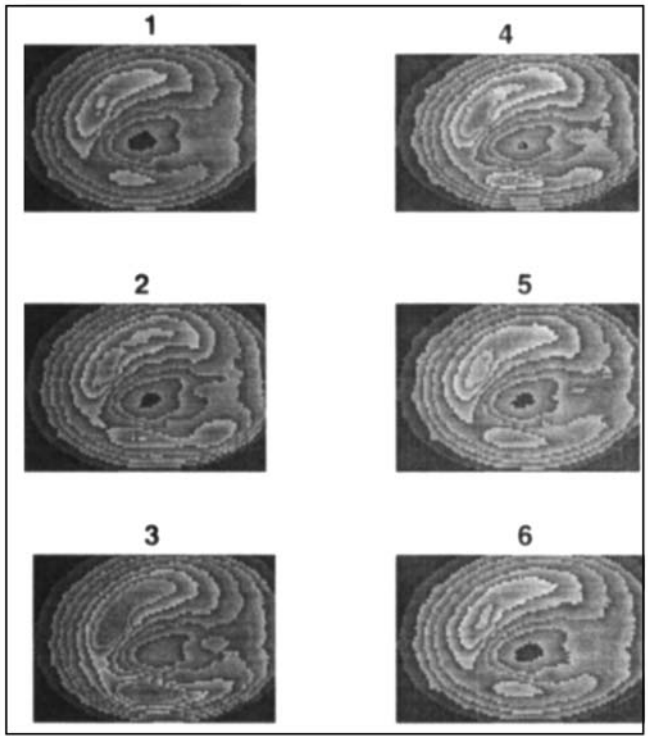

Figure 14. One cycle of periodic flickering showing the excitation of a secondary site (at the lower center part) by the primary site (hot spot at the upper left part) observed during ethylene oxidation on supported Rh catalyst.

Courtesy of Chen et al. (1993).

ences over the surface, even when all parts of the catalyst belonged to the same steady-state branch. During oscillations between the ignited and extinguished branches, different parts of the catalytic surface were oscillating independently and ignition was associated with propagation of temperature fronts over the surface.

Studying self-sustained oscillations during ethylene oxidation on supported catalysts, using IR thermography, Kellow and Wolf et al. (1991) observed that active hot zones around catalytic spots were contracting and expanding, but in most cases were not changing their position. Ignition and extinction phenomena at a particular spot could be triggered by a similar event at an adjacent spot. The reactor configuration used in their study, however, did not allow the exclusion of flow effects from the system; flow effects were evident from the fact that ignition always started at the position close to the reactor outlet and propagated inward.

Spatiotemporal dynamics on supported catalysts can sometimes be presented as the interaction of "coherent" structures induced by long-range nonuniformity. Several studies employed proper orthogonal decomposition (POD) of IR-thermographic snapshots to identify and classify the motion. Pattern dynamics was described by the linear combination of several empirical eigenfunctions. Chen et al. (1993) employed POD during ethylene oxidation on a wafer covered with Rh catalyst, to describe hot spot flickering, in which one hot-spot induced ignition of another extinct active spot (Figure 14) and hot spot wandering over the support. The ignited spot in the

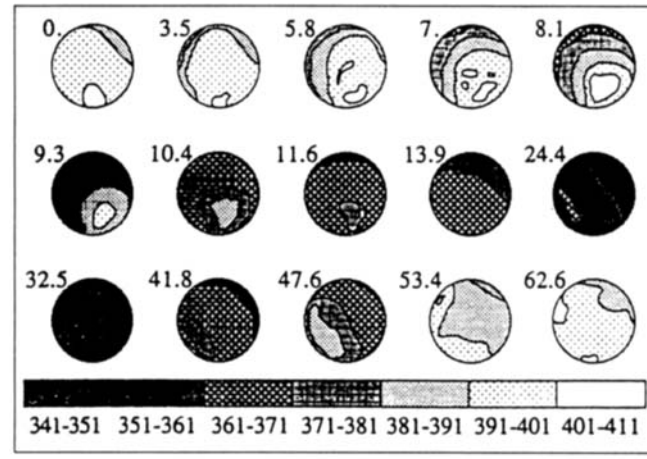

Figure 15. Thermal images observed by Graham et al. during hydrogen oxidation on a Ni disk.

Courtesy of Graham et al. (1993a).

upper left corner of the wafer ignited the extinct spot in the lower part of the surface; then, the newly ignited spot extinguished and is ignited again by the neighboring spot (Figure 14). Two- and five-term series of eigenfunctions were necessary to represent satisfactorily the observed flickering and wandering, respectively. Intermittent chaotic behavior of the conversion time-trace was attributed to perturbations, probably due to external noise, of the homoclinic trajectory of hot spot motion. The authors suggest that solutions dominated by localized structures are very likely to be observed on catalysts with long-range nonuniformity. This conclusion suggests that complete classification of patterns will remain an elusive task, but it underscores the importance of spatially resolving techniques for analyzing these patterns, since localized measurements are an inadequate measure of spatial and temporal organization in patterns dominated by several hot spots.

Lobban and Luss (1989) used IR thermography to monitor thermokinetic oscillations during hydrogen oxidation on a 3.8-cm nickel disc. Ignition and extinction occurred nonuniformly on the surface and then propagated through the entire disc. Later experiments (Lane et al., 1993) revealed two pacemakers at the edge of the disc, emitting ignition fronts that conquered the surface within 40 s. After a slow uniform cooling that was not associated with front motion, new ignition fronts originated at the pacemakers positions (Figure 15). Graham et al. (1993a) used POD for determining the basis function for the observed spatiotemporal patterns. A single cycle was successfully represented as a combination of two empirical eigenfunctions. At higher gas-phase temperatures the synchrony between pacemakers was lost, resulting in chaotic behavior.

The effect of catalyst microstructure was reported by Sant et al. (1988), who compared the behavior of two supported Pt catalysts with the same Pt loading but different crystallite size. Oscillations were absent when Pt was dispersed as big and widely separated crystallites, while a catalyst made of fine uniformly dispersed Pt particles oscillated. Partial coverage with fine Pt particles of the wafer of large Pt crystallites, which reduced the spacing between crystallites, made the former catalyst oscillate.

Plath et al. (1988) attributed the self-similar character of

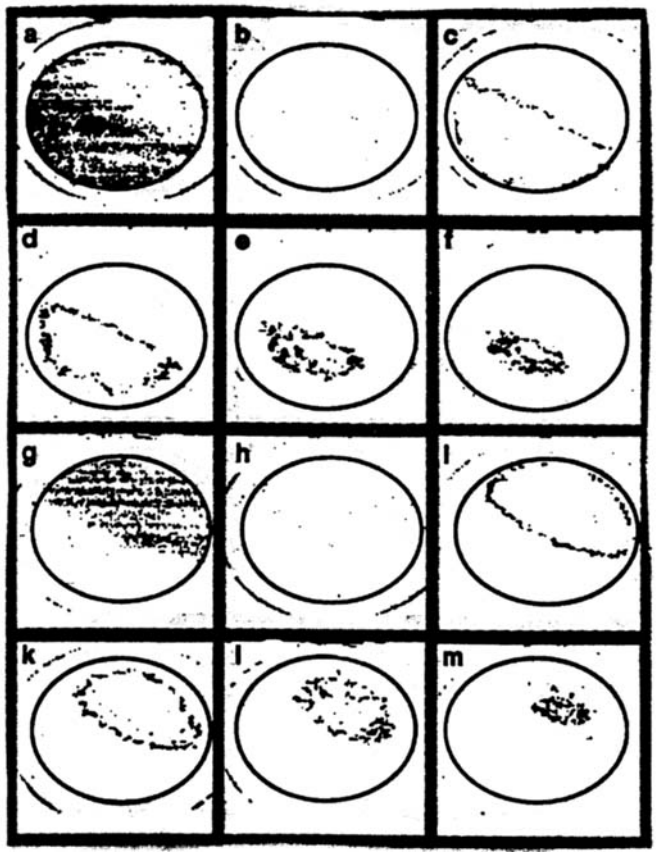

Figure 16. Spatiotemporal pattern, presented as differences of successive snapshots observed on a disc during an electrochemical reaction.

Courtesy of Hudson et al. (1993).

temporal oscillations during methanol oxidation on supported Pd to excitable wave propagation through spatial fractal media, such as alumina support. In a study of the coupling of thermokinetic catalytic oscillators during ethanol oxidation on Pd, Jaeger et al. (1986) observed periodic behavior with a uniformly catalyst-coated silver-plate; when two such plates were placed on a Teflon support within a flow reactor the oscillators were synchronized. Three catalytic discs placed in the same reactor but without direct contact between them also showed a considerable degree of synchronization.

Electrochemical Systems. Hudson et al. (1993), in a study of potentiostatic dissolution of a circular iron disc electrode, related the temporal nature of current oscillations to a spatial pattern. Period-one oscillations were associated with propagation of an approximately axisymmetric wave, which started from the rim of the electrode and propagated inward (the wave mediated the transition between passive and active states of iron). Period-two oscillations, which were observed at lower potentials, were associated with a standing wave, when two half-circles of the electrode oscillated out of phase (Figure 16).

Modeling. Collin and Balakotaiah (1994) analyzed pattern formation in a model exothermic reaction with Langmuir–Hinshelwood kinetics coupled with slow reversible and localized modification of catalyst activity. For realistic values of the ratio of heat conductivity to mass diffusivity the model could not predict stationary pattern formation. Homogeneous oscillations may become unstable, however, and traveling wave patterns may emerge. For realistic values of model parameters, the minimal system size required for pattern formation was shown to be of the order of 1 cm^2.

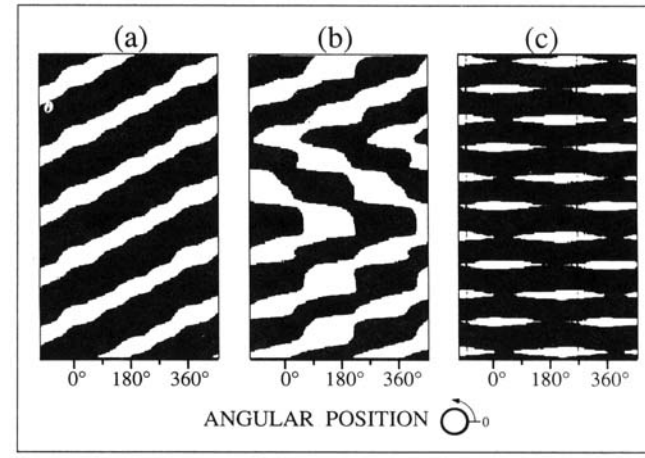

Figure 17. Temperature patterns, observed during hydrogen oxidation on a Ni ring in an atmospheric pressure mixed-reactor.

Rotating (a), rotating and alternating (b), and stationary pulses (c). Courtesy of Graham et al. (1993b). Patterns are presented in the plane of time vs. angular position.

The discrete nature of reactive sites was the incentive behind many investigations of interaction between oscillators. Jensen and Ray (1980, 1982b) simulated complex dynamics in the "fuzzy wire and pebbly surface" catalyst model, which accounted for the interaction of protrusions on a wire. Schuth et al. (1990) concluded that complex conversion oscillations during the NO + CO reaction over a supported Pd catalyst were induced by thermal interaction of several active regions on the catalyst wafer. They modeled the catalyst by 10 nonlinear identical oscillators, randomly dispersed on a 10-by-10 inert grid, which generated heat by reaction and exchanged heat with gas phase and with its nearest neighbors. Chaotic behavior emerged at intermediate values of the heat transfer coefficient to the gas phase, but the route to chaos was found to be sensitive to the distribution of active cells on the grid. Experiments with supported catalysts showed that dynamic behavior is very sensitive to the catalyst preparation.

Mixed Reactors

Observations. The global interaction between the local variables in a distributed oscillatory or bistable system and a mixed gas-phase may induce a rich structure of spatiotemporal patterns that would not exist otherwise. The global variable (e.g., gas-phase concentration) is related to the space average of the local property. This interaction is similar to the effect of an external control aimed at maintaining the average temperature (or rate) of a catalytic ribbon at a setpoint. The most spectacular examples of such interaction are the rotating temperature pulses observed during H_2 oxidation on a Ni ring (Figure 17; Graham et al., 1993b) and the standing concentration waves during isothermal CO oxidation on Pt(110) under low pressures (Figure 18; Jakubith et al., 1990).

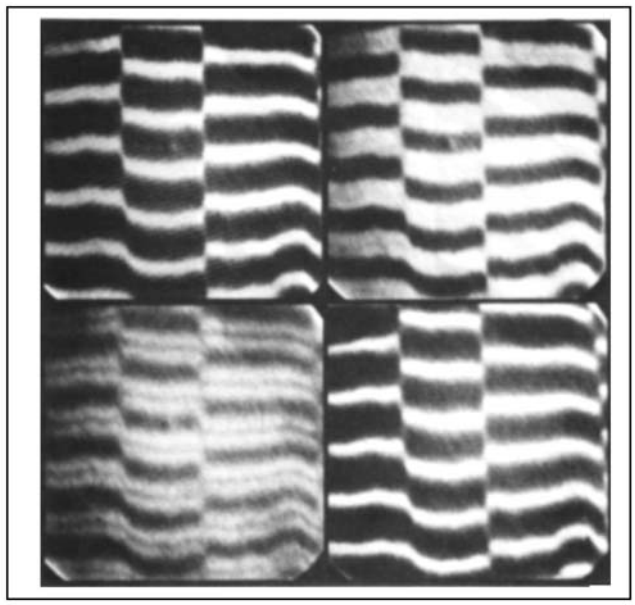

Figure 18. Standing waves associated with periodic oscillations during low-pressure CO oxidation on Pt(110).

Courtesy of Jakubith et al. (1990).

The catalytic ring in the former experiment was placed in a mixed reactor at atmospheric pressure, which in turn was placed in a fixed-temperature oven. Thus, the gas-phase temperature in the reactor was almost constant but the catalyst temperature varied (Figure 17). The global interaction of the ring, through reactant depletion in the gas phase, created the new patterns (see analysis below) presented in Figure 17 in terms of the plane of time vs. angular position. Figure 17a presents rotating unidirectional pulses, while in Figure 17b pulses expand and shrink and change direction about every 540° of rotation. Figure 17c presents stationary front patterns that resemble antiphase oscillations, except that the ring is totally extinct for sections of the cycle.

Catalytic reactions conducted at low pressures are believed to be free of mass and heat transfer resistances. Recent work attributes pattern formation in such systems to global interaction through the gas phase. The patterns observed during CO oxidation (Figure 18; Jakubith et al., 1990) show standing-wave antiphase oscillations, observed by PEEM, in which the dark and light domains represent a surface covered by adsorbed oxygen or adsorbed CO, respectively. Within the cycle the dark (or light) domain turns into light (or dark) and back again without considerable change in the front position. The coupling time was estimated to be 10^{-2} s, compared with a mixing time of 10^{-4} s.

The impact of global coupling on pattern formation, during the reaction of NO and CO on a Pt(100) surface at 10^{-6} torr in a gradientless flow reactor, was recently reported by Veser et al. (1994) and modeled by Mertens et al. (1993). In this case, the extent of surface reaction is very sensitive to the absolute coverages, which in turn depends on the gas-phase conditions and is very close to the critical value that induces surface-phase transition between the hex and 1*1 phases. Thus, slight variations of the partial pressures (reported to be $\sim 1\%$) change the extent of surface reconstruction, yielding an efficient mode of global coupling. With decreasing catalyst temperature the global coupling collapsed, as evident by surface (PEEM) images and by the discontinuous drop in the reaction-rate amplitude. This was attributed to the presence of surface defects. Lowering the temperature led to increasing difference between frequencies of oscillations due to defects and those due to uniform surface. Beyond a critical temperature value, the defects ceased to be entrained by the uniform oscillations of the globally coupled surface and started emitting waves at their own frequency. When the surface was conquered by these traveling waves, the spatial average of the reaction became constant in time, and thus the impact of global coupling was reduced.

Kapicka and Marek (1989) observed complete synchrony between pellets in a high-recirculation packed-bed reactor, during CO oxidation over supported Pt catalyst; the amplitudes and form of oscillations differed from one pellet to another. Temporal patterns became more complex at higher temperature; significant concentration gradients existed at low recycle ratios, but the pellets were synchronized.

Modeling. In order to study the effect of global coupling on pattern selection in a catalytic ring, Middya et al. (1994a) analyzed a catalyst-reactor condensed model, of the form shown in Eqs. 8b, 8c and 9 with cubic nonlinearity. They also showed that in an isothermal-fluid reactor of small volume (i.e., residence time), the global variable—the gas-phase reactant concentration (λ)—is related to the average temperature like $\lambda = B(T_s - \langle T \rangle)$. Patterns are formed when the fluid temperature is constant, but the catalyst temperature and reaction rate ascend with increasing reactant concentration, so that the changes in reactant concentration in the vessel tend to arrest moving fronts. Recall that we have classified such solid–fluid interaction as symmetry breaking. The sensitivity parameter (B) is inversely proportional to feed flow rate and patterns are formed since the feed rate is insufficient to maintain the ignited state, yet it is larger than the reactant consumption rate at the extinguished state. Note that symmetry breaking will occur due to fluid-phase interaction, even in a single-variable bistable problem (fixed y), as it does in controlled catalytic wire. The reactant concentration will be self-adjusted then to maintain a stationary front and the front position will match the mass balance on the fluid phase.

In the limit of infinite B (very small flow rate) the problem is identical to a wire subject to constant resistance control

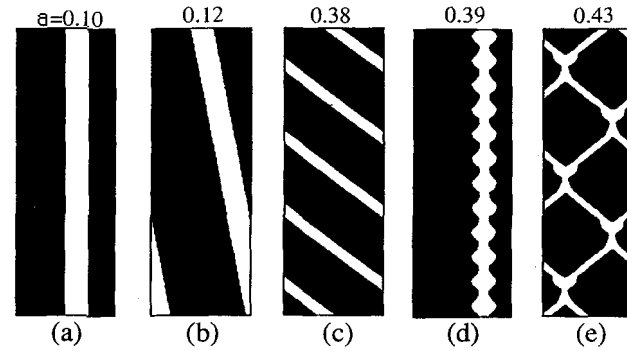

Figure 19. Simulated patterns in a catalytic ring subject to global interaction.

Stationary (a), rotating (b), (c), stationary but breathing (d), and crossing (e) pulses. Courtesy of Middya et al. (1994a).

($\langle T \rangle = T_s$) and the main patterns were outlined in the corresponding section. Here we also consider the possible motion on a ring, since patterns may be induced by interaction via a mixed fluid phase, while constant-resistance control cannot be applied to a catalytic ring in a simple way. Moving patterns in a ring include (Figure 19; Middya et al., 1994a):

- Unidirectional pulses that move at a constant velocity around the ring. This motion may consist of one (Figure 19b) or several pulses (Figure 19c) on the ring. This motion is possible even without global interaction ($B = 0$), but its attainment requires certain nonuniform initial conditions, and it may be difficult to experimentally achieve such a state only by varying the feed conditions.
- Source point, from which two pulses emerge periodically and travel until their annihilation at another point and the creation of a new source point at the initial location.
- Crossing pulses are pairs of pulses that move in opposite directions and cross (or reflect from) each other (Figure 19e).
- Rotating antiphase oscillations.
- Stationary (Figure 19a) or breathing (Figure 19d) pulses.

Let us compare the patterns observed in the two simple one-dimensional geometries, a ribbon and a ring. Patterns found for a ribbon geometry, such as antiphase oscillations (Figure 11c), have not been predicted to occur in a ring. Furthermore, patterns that reflect the existence of system boundaries (e.g., a pulse that reverses its direction; Figure 11f) are not expected to exist in a ring geometry unless artificial boundaries are constructed. Within the domain of stable homogeneous solutions, uniform initial conditions lead to homogeneous stable or oscillatory solutions. A rotating pulse in a ring can be attained either by crossing the stability boundary of the homogeneous solution (by varying B) or by an inhomogeneous perturbation. In the absence of interaction between a global lumped-variable λ and the surface-state variables ($B = 0$), there exists a stable homogeneous solution for any Z. Numerical simulations of motion on a ring verified that once unidirectional (UD) pulses are attained they are stable over a wide domain of parameters, even without global interaction; that is, a rotating pulse may coexist with a stationary or oscillatory homogeneous solution. The achievement of other patterns that may coexist usually requires either a large perturbation of the UD pulse or a slow change of parameters from a region in the space in which the specific pattern is known to exist. On a ribbon, on the other hand, neither the UD pulse nor any pattern can be sustained without global interaction. There is no predominant pattern on a ribbon. Uniform initial conditions lead either to a homogeneous solution or to a pattern when the homogeneous states are unstable. The domain of the existence of the patterns shrinks with decreasing B. A map of the regions with qualitatively different patterns was constructed in the plane of interaction strength vs. system length (Middya et al., 1994a).

The standing concentration waves observed during low-pressure CO oxidation clearly suggest that global coupling effects are important. The high wavenumber in this study is intriguing since coupling by a mixed variable typically generates one front or one pulse patterns (e.g., Figures 11 and 19). Levine and Zou (1993) and Falcke and Engel (1994) have analyzed the pattern formation in this system using the detailed mechanism of this reaction on Pt(110) plane and a gas-phase balance. This model is qualitatively similar to the one described earlier except that in the low-pressure studies the gas-phase volume is large and a pseudo-steady-state assumption is not invoked for the reactant concentration. Stable multiwave patterns were simulated to exist over a narrow range of parameters. Several studies (Mertens et al., 1993) have employed a modified CGL equation to qualitatively account for patterns due to global coupling. In the presence of "defects" this model accounts for the observations made during the reaction of NO and CO: there existed a critical difference between the frequencies of the "defect" and of the uniform surfaces above which the global coupling collapsed, leading to the discontinuous decrease of the averaged amplitude of global oscillations and accompanied by a sharp increase in the frequency of local oscillations.

Discrete Systems. Cell approach, which envisions the catalytic reactor as an array of coupled cells, was applied for the description of supported catalysts and nonuniformly activated wires in many experimental and theoretical studies. Brown (1985) showed that the various reaction-rate branches, observed during hydrogen oxidation in a mixed reactor with few catalytic pellets, correspond to a patterned state. Thermographic investigation of the catalyst surface indicates that in most cases multiple hysteresis cycles are caused by a patterned solution in which only part of the catalyst (wire, particle assemblage) is ignited. Arce and Ramkrishna (1991) have shown that fluid mixing in a reactor with few catalytic pellets can be responsible for pattern formation even in the absence of direct particle interaction: such interaction may induce a unique solution in the reactor even when multiple solutions exist for a single particle. Studies of coupled BZ reactors and interacting heterogeneous catalytic oscillators have shown, both theoretically and experimentally, that the interaction can lead to rhythm splitting, entrainment, and oscillator death phenomena. Kim and Hlavacek (1986) showed that a coupled pair of CSTRs, which are oscillatory in the absence of interaction, may become steady due to the coupling. The domain of coupling coefficients that induce steady-state operation was found to increase with increasing differences between two oscillators. Several experiments have demonstrated that coupling may induce oscillatory behavior in two units that are individually stable (Boukalouch et al., 1991, studied two asymmetrically fed coupled CSTRs; Wang and Hudson, 1992, and Bell et al., 1992, studied two rotating electrodes).

Fixed-Bed Reactor

While catalytic wires, rings, and discs are simple one- and two-dimensional model systems that lend themselves to comparison with theory, the workhorse of the catalytic process is the fixed bed. Qualitative and quantitative analyses of spatiotemporal patterns that may arise in a one-dimensional fixed-bed reactor are important in order to develop the methodology for motion identification and classification. These analyses help to elucidate possible characteristic motions in the reactor and implement necessary adjustments or control of reactor operating conditions. This problem may be of crucial importance for expediting the startup of a cold catalytic converter.

We review below experimental observations of front propagation, multiple solutions, and oscillatory behavior in a fixed-bed reactor. While some of these results can be, and were, described by a homogeneous model, which we do not

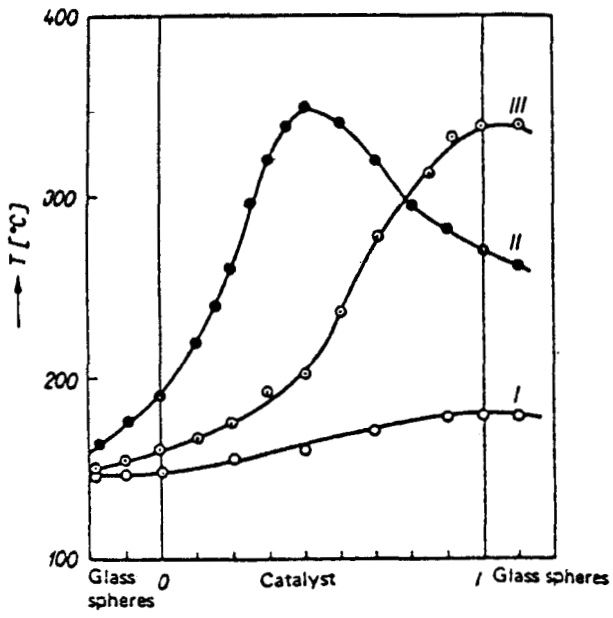

Figure 20. Triplicity of temperature profiles observed in a 8.9-cm bed packed with $CuO/\gamma Al_2O_3$ during CO oxidation.

Courtesy of Votruba and Hlavacek (1972).

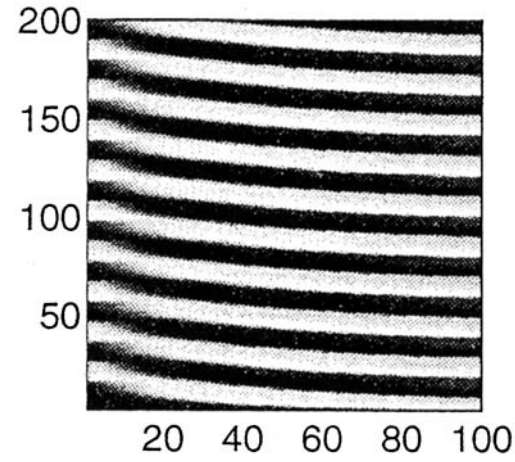

Figure 21. Spatiotemporal patterns exhibited by u_t-u_{zz} $=-u^3+u+\lambda_{in}-\int u\,dz$, subject to no-flux conditions at $z=0$ and $z=100$ and $\lambda_{in}=0$.

This single-variable model qualitatively describes the interaction of convection, reaction, and diffusion (conduction) in a reactor with a continuous reactant supply (Sheintuch and Shvartsman, 1994).

review in this work, this identification in the cases listed below is not unambiguous.

Fronts

Creeping reaction zones, first reported by Wicke and Vortmeyer (1959) and Frank-Kamenetski (1969), are encountered typically in response to a step change in operating conditions. Since a pseudohomogeneous adiabatic bed catalyzing an exothermic and activated reaction can exhibit a steep temperature profile, changing feed conditions induces a creeping front motion. Typical creeping velocities are small, 10^{-5} m/s in order of magnitude (Sharma and Hughes, 1979; Paspek and Varma, 1980; Puszynski and Hlavacek, 1980) due to the small solid-phase conductivity. Simon and Vortmeyer (1977) used a homogeneous reactor model for predicting and calculating creep velocities in a bed catalyzing ethylene oxidation. Creeping fronts are not necessarily fronts that connect two different solutions of the local steady-state problem. Proper characterization of spatiotemporal motion in a fixed bed requires knowledge of the local (single-pellet) solution, and this information was absent in most studies of fixed-bed dynamics. This information is also essential for determining the dynamic response to external perturbations. In the domain of steady-state multiplicity a perturbation of one state may trigger the transition to the other state; the transient typically takes the form of a front that creeps from initial to final position, leaving the system behind in a new steady state.

Bistable kinetics

Observations. Global steady-state multiplicity may be accounted for by a homogeneous reactor model due to axial dispersion (Hlavacek and Van Rompay, 1981) or by a heterogeneous model of a plug-flow reactor showing local bistability due to thermal or kinetic effects (Sheintuch, 1987). Most experimental studies did not discriminate between the two mechanisms by studying the local behavior. We list below, therefore, the main observations of steady-state multiplicity in fixed beds irrespective of their origin. Experimental studies typically report two stable global solutions in which the whole reactor operates either in the kinetic or in the diffusion regime (e.g., Wedel and Luss, 1984, in a study of CO and CO_2 methanation). Triplicity was observed by Votruba and Hlavacek (1972) during CO oxidation in an adiabatic CuO/Al_2O_3 reactor (Figure 20): the low temperature state is fully extinguished, while the intermediate resembles a stationary front. Multiplicity of five stable solutions was observed during CO oxidation in a Pt/Al_2O_3 bed (Hegedus et al., 1977). This large number of solutions suggests that other solutions exist but were not detected. Adjaye and Sheintuch (1990) traced four branches of steady-state solutions during ethylene oxidation in an adiabatic bed of alumina-supported Pt catalyst; all states exhibited a sharp front near the reactor inlet with small variation in the temperature downstream from the front. A single pellet was shown to exhibit only two steady states.

The transient from one global steady state to another was demonstrated by Sharma and Hughes (1979) in their study of an adiabatic fixed-bed reactor packed with CuO/SiO_2 catalyzing CO oxidation: a pulse change in the inlet concentration of CO led to the establishment of a diffusion-controlled regime in an initially extinguished reactor. Puszynski and Hlavacek (1980, 1984) observed multiplicity of creeping profiles: the direction of front propagation was dependent on initial conditions. This is characteristic of front propagation in a heterogeneous reactor with a locally bistable media, as one can ignite the extinguished state or vice versa.

Modeling. The heterogeneous reactor model with local bistable kinetics predicts infinitude of solutions when heat conduction along the bed is neglected. (Rhee et al., 1973); this is a structurally unstable feature, as the incorporation of a conduction (or diffusion) term induces front propagation.

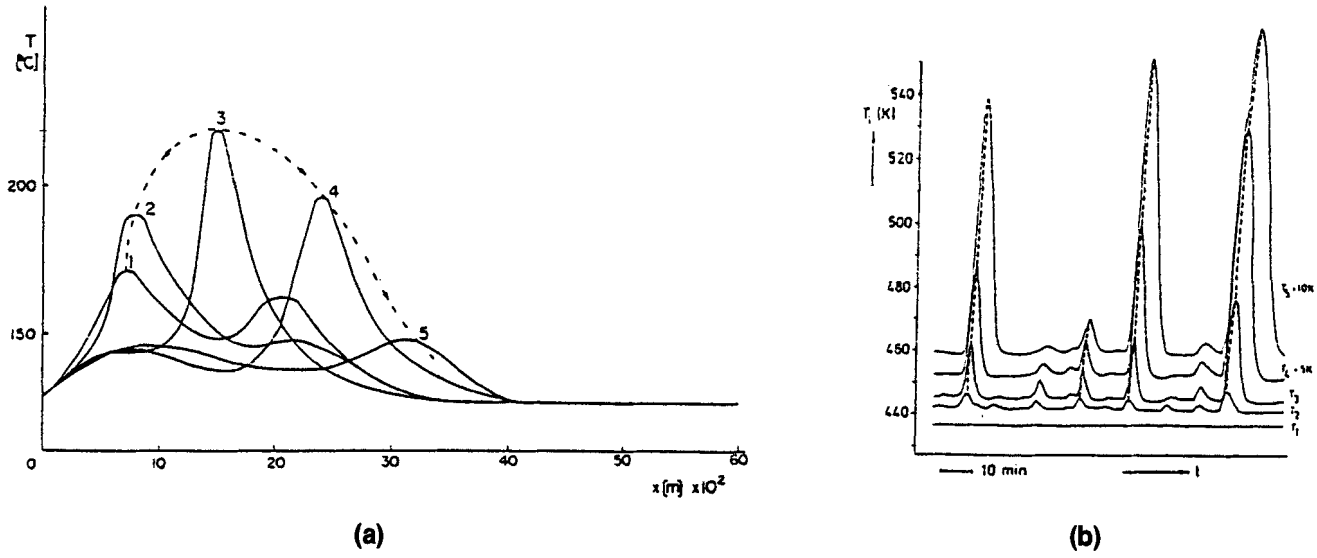

Figure 22. Oscillatory patterns observed in a fixed-bed reactor during CO oxidation.

(a) Pulse birth, motion, and exit in a nonadiabatic bed (courtesy of Puszynsky and Hlavacek, 1984). (b) Oscillatory motion due to amplification of small fluctuations at the inlet (T_1) with flow downstream (courtesy of Onken and Wicke, 1986).

The front(s) may exit the system or become stationary, and typically only a few steady-state solutions are possible (Eigenberger, 1972; Rhee et al., 1974). Aside from the fully ignited or fully extinguished states, the heterogeneous model may create a stationary front solution (Sheintuch, 1987). Fluid conditions at the front position correspond to front stationarity (Eq. 15) and the front typically separates an extinguished domain upstream from an ignited one downstream. The solution is stable since a small displacement of the front position (say, downstream) will induce conditions (higher fluid temperature) that counteract the original perturbation.

Motions in a fixed bed with bistable kinetics are not limited to multiple states. The interaction of thermal multiplicity and reactant flow may induce a periodic sequence of upstream-moving pulses. To demonstrate this motion we simulated and analyzed the behavior of the single-variable (fixed y) condensed model (Eq. 8), which can be written as an integrodifferential equation of the form

$$u_t - u_{zz} = f(u, \lambda) \tag{27a}$$

$$u_z(0,t) = u_z(L,t) \tag{27b}$$

$$\lambda = \lambda_{in} + \int_0^z \frac{g(u)\,dz}{U}. \tag{27c}$$

Let us define λ so that $f = 0$ is S-shaped in the (u, λ) plane. The necessary conditions to exhibit patterns, then, are that the system exhibits symmetry-breaking interaction between the phases and that $g(u)$ should change sign so that $g < 0$ (> 0) on the upper (lower) branch of the $f = 0$ nullcurve. To obtain nonmonotonic dependence of $g(u)$ another source or sink, in the form of a second reaction or of an evenly distributed supply or removal of mass or enthalpy, is necessary: In an adiabatic reactor such behavior is possible when a second consecutive endothermic and highly-activated reaction occurs so that heat is adsorbed at high temperatures and produced at low temperatures. In an isothermal reactor oscillatory behavior will emerge if the reactant to the main reaction is produced by another reaction or supplied through the wall (i.e., a membrane or cross-flow reactor) at a constant rate that is intermediate between the consumption rates at the two branches of the main reaction.

The main motions in such a reactor can be demonstrated with a cubic reaction generation function, $f = -u^3 + u + \lambda$, and a linear $g(u) = -u$ one. Typical solutions for $\lambda_{in} = 0$ show successive pulses that are generated at the reactor outlet (at the right-hand side, Figure 21) and move upstream. The behavior will be similar for any other $f(u, \lambda)$, $g(u)$ that obeys the preceding conditions and when $\lambda = 0$ is the fluid-variable for which diffusion-reaction fronts are stationary. Further analysis and approximate solutions are presented by Sheintuch and Shvartsman (1994).

Oscillations and excitability

Observations. Self-sustained dynamic behavior, in the form of successive birth and propagation of ignition and extinction fronts, was reported by Puszynski and Hlavacek (1984) in a nonadiabatic reactor catalyzing CO oxidation. In the region of global monostability a hot spot emerged at the reactor inlet, propagated toward the outlet at an average velocity of 10^{-4} m/s, and died out as another hot spot was born at the inlet (Figure 22a). A similar behavior was observed with the same reaction in an adiabatic fixed bed (Wicke and Onken, 1988): A hot front emerged at the reactor inlet and moved downstream as its amplitude increased (Figure 22b). A single catalytic pellet, when subject to the inlet ambient conditions, was shown to exhibit small-amplitude thermokinetic oscillations. The authors suggest that at the border between local mono- and bistability these oscillations may be strongly amplified by triggering successive fronts.

Sheintuch and Adjaye (1990) and Dvorak et al. (1993) observed motions of excitable waves in response to a local perturbation at the inlet of an adiabatic reactor catalyzing C_2H_4 or CO oxidation, respectively. Setting a local perturbation at

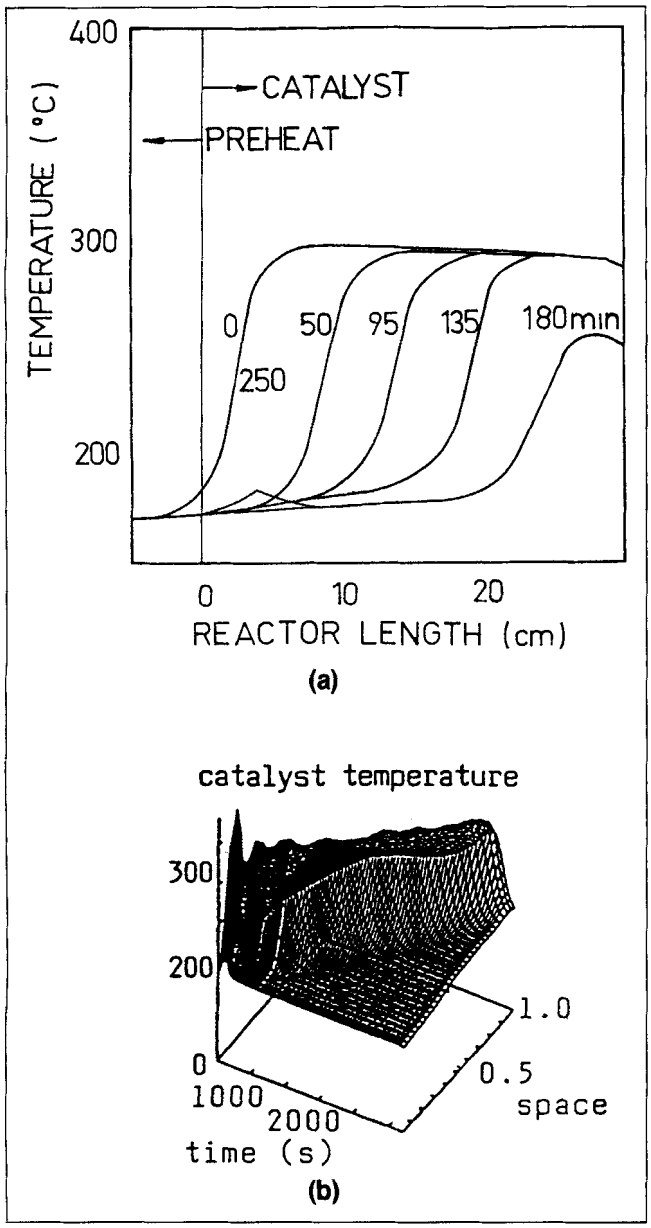

Figure 23. (a) An excitable wave in an adiabatic fixed-bed catalyzing ethylene oxidation: perturbation of the upstream section sends a front that travels and exits the reactor while a new front appears at the inlet (Sheintuch and Adjaye, 1990); (b) pulse motion after setting a local ignition to the feed section of an adiabatic bed during CO oxidation.

Courtesy of Dvorak et al. (1993).

the inlet of a 30-cm-long bed packed with Pt/Al_2O_3 catalytic pellets induced a front that moved at constant speed and shape, in the case of ethylene oxidation (Figure 23a). The front always moved downstream until its exit. A hot spot then appeared at the inlet (at 180 min; Figure 23a). It developed and spread across the reactor, and the old steady state was established (see Sheintuch, 1990b, for the qualitative analysis of this transient). In the case of CO oxidation, local heating of the reactor inlet, or of an intermediate position, created an ignition front that propagated at constant speed through the bed followed by the extinction front (Figure 23b).

Modeling. We focus our attention now on typical motions that may emerge in a heterogeneous model of a fixed bed with oscillatory kinetics. While a homogeneous thermokinetic model (i.e., one with C_f and T_f as its dynamic variables) may exhibit oscillatory behavior, it does so for unrealistic values of parameters and predicts unrealistically fast oscillations. The motions in the fixed-bed reactor differ from those in a uniform medium due to the convective flow and the effects of reactor boundaries: the local conditions in the bed (fluid concentration and temperature) vary in conjunction with the state of the system (extinguished or ignited) and the local state of a single pellet (i.e., the corresponding phase plane) may vary from an excitable one, upstream, to an oscillatory one, downstream. Two groups recently studied extensively the motions in a fixed-bed reactor. We studied the dynamics of a heterogeneous reactor model that accounts for a local (solid-phase) oscillator and a global (gas-phase) convective interaction: Rovinski and Menzinger (1992, 1993) (see below) analyzed a model in which the activator or the inhibitor was moving while the other variable was immobile.

Barto and Sheintuch (1994) analyzed the behavior of a detailed adiabatic-bed model in which an exothermal reaction occurs. The local oscillator, similar to that employed for studies of global interaction, incorporated a fast and diffusing surface temperature and a localized activity as its dynamic variables. Pattern selection was determined by the nature of interaction between the phases, by the phase planes spanned by the reactor, and by the ratio of the two slowest time scales: front residence time and the period of oscillations. In an adiabatic reactor with exothermic positive-order oscillatory reactions, or in other reactors with symmetry-preserving interaction, the common patterns are as follows:

- Excitable behavior is realized when a local perturbation is applied to the outlet (Figure 24a) or to the inlet (Figure 24b) of a bed lying in the excitable domain. When the bed is initially ignited, the excitation will send a trigger front that

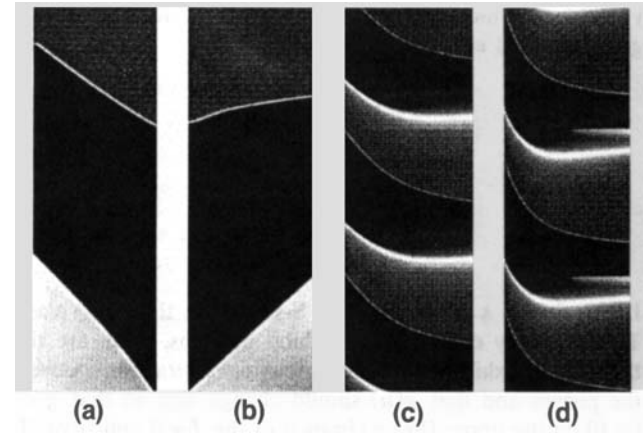

Figure 24. Spatiotemporal patterns, simulated with an adiabatic fixed-bed reactor model, showing excitable wave motion, after setting a local extinction to the inlet (a) or exit (b) section, and simple (c) or complex (d) periodic patterns.

Courtesy of Barto and Sheintuch (1994).

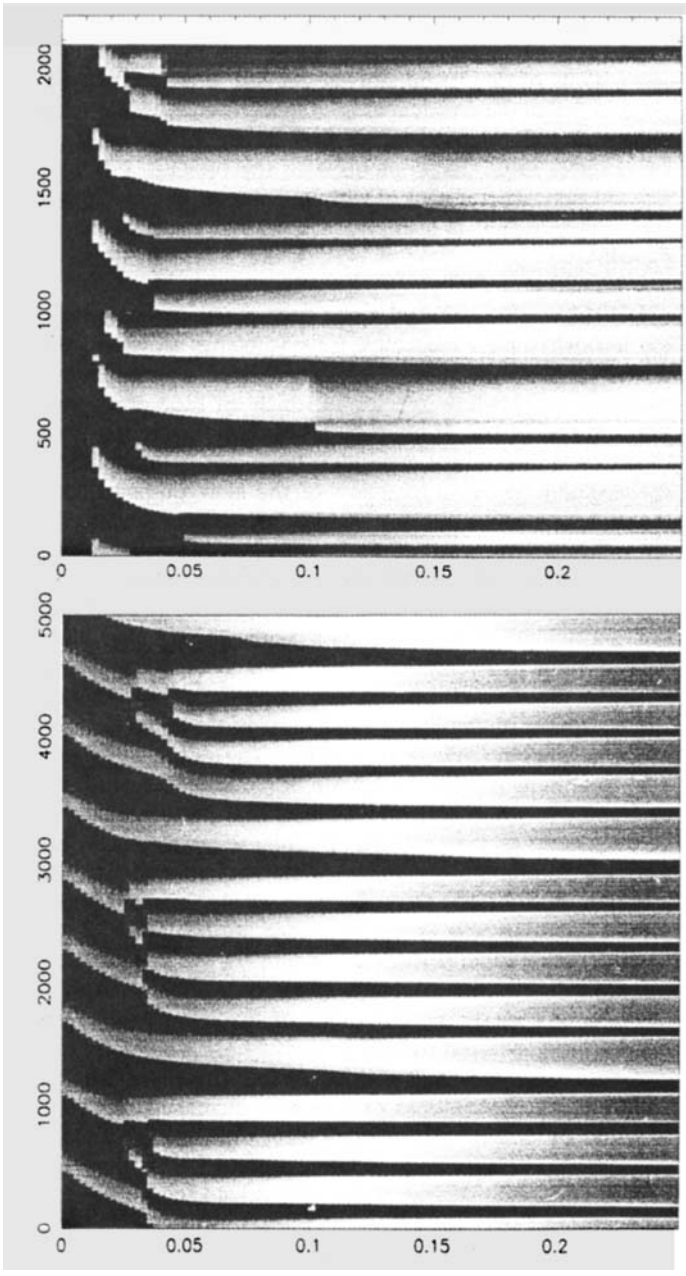

Figure 25. Aperiodic split-band (top) and coalescing-band (bottom) patterns simulated with an adiabatic fixed-bed reactor model.

Courtesy of Barto and Sheintuch (1994).

sweeps through the bed, followed by a relaxation back into the ignited state and a second trigger (Figure 24a) or phase (Figure 24b) front. Figure 24b accounts for the observation made during ethylene oxidation (Figure 23a) that the initial slow front is induced by conduction while the consecutive fast front is mediated by convection.

- Almost homogeneous oscillations (periodic horizontal bands) emerge when the inlet is oscillatory; when the inlet is excitable, but the outlet is oscillatory, periodic (parallel band, Figure 23c) patterns emerge with upstream-moving fronts that move fast through the downstream section and slow down as they reach the inlet.

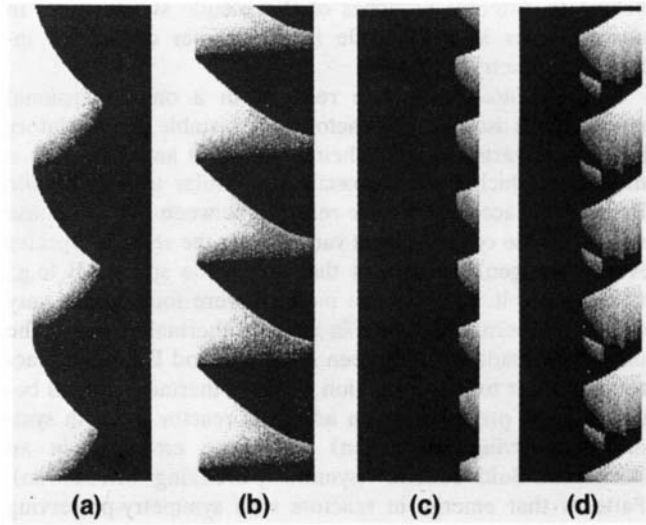

Figure 26. Spatiotemporal patterns simulated for an isothermal reactor with oscillatory kinetics.

Oscillatory fronts (a), (b), and simple (c) or complex (d) sticking fronts. Courtesy of Shvartsman and Sheintuch (1994).

- Upstream-moving pulses emerge when the inlet is oscillatory but the outlet is nonexcitable.
- Stationary, oscillatory, or sticking fronts emerge when the system spans the bistability region. In the latter pattern the front originates at the outlet and moves upstream before turning around and disappearing (similar to Figure 26c).
- Split-band-patterns appear when new fronts are generated inside the reactor, but they cannot propagate due to the refractory trail of the previous pulse. They form multiperiodic (Figure 24d) or aperiodic (Figure 25a) sequence of pulses; the understanding of the transition between these multiple structures has not been achieved yet. Successive coalescence of fronts, as they move upstream, may also generate an aperiodic pattern (Figure 25b).

A finite difference scheme was employed to solve the detailed model described earlier, using realistic widely separated time and length scale parameters. Numerical solutions of this type are too computer-time-consuming to screen the parameter space. To overcome the computer-time constraints Shvartsman and Sheintuch (1995) classified the main spatiotemporal patterns in one-dimensional reactors and extended the simulation into two-dimensional models using simplified kinetics and integration procedures. The phase plane was approximated by a piecewise linear model, while the numerical scheme (Barkley, 1991) utilized time-scale separation and is a numerical equivalent of the singular perturbation approach to the problem. A model similar to this one was used to simulate the properties of spiral waves during low-pressure CO oxidation on Pt (Bar et al., 1994). The behavior of an adiabatic reactor was analyzed, as well as that of an isothermal-fluid reactor in which the fluid temperature is constant but the solid temperature varies due to reaction. Motions in an adiabatic reactor were similar to those of the exact model (Barto and Sheintuch, 1994). The main difference between adiabatic and isothermal-fluid PFR is that in the latter convection induces symmetry breaking (in the sense that it favors solutions in which different parts of a reactor

belong to different branches of the pseudo steady state) in positive-order kinetics, while in the former convection inhibits asymmetry.

Similar patterns may be realized in a one-dimensional model of an isothermal reactor with bistable or oscillatory kinetics. Shvartsman and Sheintuch (1994) analyzed such a model, in which the local oscillator, similar to a reversible Brusselator, accounts for the reaction between two gas-phase species whose concentration varies along the reactor: Species A (e.g., oxygen) accelerates the rate, while species B (e.g., CO) inhibits it. Many of the patterns were found to be very similar to thermal patterns in a nonisothermal reactor. The distinction made here between A-limited and B-limited reactors is similar to the distinction made in thermal patterns between those produced in an adiabatic reactor (or with symmetry-preserving interaction) and those emerging in an isothermal-fluid reactor (symmetry-breaking interaction). Patterns that emerge in reactors with symmetry-preserving interaction were described earlier (see also Figures 26c and 26d). A PFR with symmetry-breaking interaction may exhibit the following motions:

- Upstream- or downstream-moving pulses (parallel bands) or source points (V-shaped bands) emerge when the system spans the oscillatory domain; if the inlet or outlet are not excitable, the pulses terminate short of the inlet or outlet, respectively.
- Stationary or oscillatory (Figure 26a) fronts emerge when the bistability domain is spanned; the amplitude of the front oscillations in the latter pattern may span the whole reactor (Figure 26b).

The patterns outlined earlier can also be predicted by the condensed model (Eq. 8) using simple cubic kinetics (Sheintuch and Shvartsman, 1994). For the PFR asymptote, the model takes the form

$$u_t - u_{zz} = -u^3 + u + v + \left(\lambda_{\text{in}} + b\int_0^z \frac{(u+u_0)}{U}\,dz\right) \tag{28a}$$

$$u_z(0,t) = u_z(L,t) \tag{28b}$$

$$\frac{1}{\epsilon} v_t = -\alpha u - v. \tag{28c}$$

The cases with $b = 1$ or -1 correspond to symmetry-preserving or symmetry-breaking interaction, respectively. Recall that this model also accounts for the case where mass (as well as heat) is supplied or removed along the reactor, for example, through a membrane, so that the fluid variable need not necessarily be monotonic; this case, which was modeled by choosing $u_0 = 0$, did not reveal new motions, different from those predicted for a bistable system (Figure 21), except that for large α the solution may become multiperiodic.

Rovinsky and Menzinger (1992) suggested that disengagement by differential transport may be accomplished not only by the difference in diffusivities of the two variables but by the differential flow of these variables as well. They have demonstrated this DIFICI by analyzing the condensed model with a flowing activator and localized inhibitor (Eq. 10). The model may admit a homogeneous solution and is amenable to linear stability analysis aimed at deriving the critical flow rate that induces this instability. Sustained patterns may be realized only when the instability feeds itself by imposing periodic boundary conditions, which are highly unrealistic for fixed beds, or by incorporating a recycle stream. Numerical simulations of the Pushinator model with a differential flow term in a one-dimensional ring-shaped reactor, yielded traveling waves that moved in the flow direction (Rovinsky and Menzinger, 1992). Experiments with the oscillatory BZ in a straight tube reactor packed with immobilized ferroin showed that a system that is stable in a quiescent medium may be destabilized by the flow of one of the reactants (Rovinsky and Menzinger, 1993).

DIFICI may be induced when both reactants are flowing, but also when their respective wave velocities are sufficiently different. Yakhnin et al. (1994) considered a homogeneous model of a cross-flow reactor in which an exothermic reaction was conducted. Homogeneous oscillations are not possible when the solid heat capacity is large, but patterns may be realized due to the interaction of the slow propagation of thermal waves with the fast motion of reactant waves. This difference is known to induce "wrong-way behavior" in realistic fixed-bed models. Patterns are obtained when periodic boundary conditions are imposed, or when inlet concentration and temperature are varied periodically, but they disappeared when conventional Danckwerts conditions are applied. In the absence of feedback of perturbations, this system is capable of amplifying small oscillations in the feed, but will not generate sustained patterns. The necessity of periodic conditions for the emergence of patterns was confirmed by Dawson et al. (1994), who showed that perturbations will be dampened at any particular position while they grow in a traveling coordinate system, or in the direction of the flow. Yakhnin et al. (1995) showed that a reactor subject to convective instability acts as a filter for the random noise applied to the reactor inlet, selectively amplifying the perturbations corresponding to the maximum of the dispersion relation. In the case of periodic perturbations of the input parameters, the reactor generated traveling waves whose wave amplitude increased downstream. It is possible that this instability may account for the wave-train pattern with increasing amplitude reported by Onken and Wicke (1986; Figure 22b). Sangalli and Chang (1994) studied the interaction of DIFICI and Turing instabilities, and showed that it may lead to spatiotemporal chaos.

Concluding Remarks

Spatiotemporal patterns should be common to many catalytic (especially oxidation) and electrochemical reactions since these classes of reactions exhibit nonlinear kinetics. The detection and classification of patterns is challenging academically as well as rewarding technically. The preceding review demonstrated that patterns in high-pressure systems typically emerge due to global coupling and are distinctly different from classic reaction-diffusion patterns. The identification and classification of patterns are important for design and operation procedures, as these reactions are employed in pollution-abatement processes and in alternate fuel production. We tried to present a comprehensive classification of patterns by considering reactors of increasing degrees of complexity: a wire or ribbon exposed to uniform conditions, a globally coupled catalyst in a mixed reactor or in a control loop, and a fixed bed in which coupling by convection occurs only in one direction. While the mechanism of catalytic oscil-

lations at high pressures is still being debated, the similarity of the patterns simulated for various detailed and condensed models along with qualitative understanding of the motion, suggests that these patterns are highly insensitive to the kinetic details, provided that the relation among the length and time scales are maintained.

Future research into catalytic patterns should focus on two targets: (1) the study of realistic models of catalytic (e.g., pollution-abatement) processes, to determine the implication of pattern formation and front motion on design and control and to verify these motions experimentally, and (2) the study of pattern formation due to global coupling, mainly in two- and three-dimensional systems. A target that remains elusive at this stage is the exploitation of spatial patterns in order to enhance reactivity, selectivity, or catalyst activity.

A realistic model for CO and olefins oxidation in a catalytic converter, which is necessary in order to optimize the startup of a cold converter, should account for thermal effects, for temperature and concentration gradients between the phases, and for the nonlinear kinetics of surface reactions. Recent designs employ resistive heating in order to expedite the startup of a cold converter (Oh et al., 1993). Such heating can be applied locally, in order to produce a traveling front, or globally (using a metallic monolith) to heat up the whole reactor or its part. With limited (battery) power such heating should be optimized to determine the distribution of power input in space and time. Since a local perturbation may produce a sustained traveling pulse, an optimal heating policy may be obtained by periodic local perturbations at the inlet or the outlet. Another process likely to exhibit pattern formation is the reverse-flow reactor, in which the feed is periodically switched between the two edges of a fixed bed. The desired solution is a stationary thermal pulse, or an oscillatory pulse of small amplitude of displacement. The behavior is usually accounted for by a heterogeneous model (Rehacek et al., 1992). The class of reactions for which this process is applied, namely catalytic oxidation on noble metal catalysts, can exhibit complex behavior. It may be of interest to study the design conditions (switching time) for excitable or oscillatory media. A recent study of ethylene oxidation on Pt/Al_2O_3 in a circulating-loop autothermal reactor revealed complex dynamics associated with periodic front motion (Laushcke and Gilles, 1994).

Control of heterogeneous reactors in which the catalytic phase can sustain spatiotemporal patterns is another novel problem. Recent efforts were aimed at suppressing oscillatory behavior caused by fronts moving in the solid phase: Qin et al. (1994) used feedback control to suppress the hot spot motion in order to eliminate the space-averaged oscillations during CO oxidation on a supported catalyst. Qin and Wolf (1994) applied vibrational control to the same system in order to achieve higher conversions in the oscillatory regime.

The problem of pattern-formation due to global interaction has established itself as a realistic and rapidly developing area of research. Several such mechanisms, due to the interaction of convection-conduction and reaction, has been reviewed here, and other models of pattern formation are expected to emerge. Analytical results are still lacking for many problems of global interaction. Analytical work for an ensemble of oscillators may be possible in the extreme situations of a system with widely separated time and length scales and in a system close to the Hopf bifurcation (the Ginzburg–Landau equations). The advantage of such analysis is the expected universality of behavior. The former approach is valid for many catalytic systems that exhibit relaxation oscillations. Scale separation is necessary for the description of traveling fronts and pulses. Future studies of one-dimensional systems should understand the transition between patterns and the transition to aperiodicity and spatial chaos. Work on two-dimensional discs and foils subject to global interaction, via the fluid phase or by control, should unravel the characteristic patterns and their differences from those obtained in one-dimensional systems. Several two-dimensional limiting models of the three-dimensional packed beds can be considered. In the annular-cylinder reactor each longitudinal position is a ring that may sustain moving patterns. In the full bed, when angular symmetry is assumed, one can envision an excitable wave in the form of an expanding ring that propagates downstream, after a local perturbation is applied at the center of the inlet plane. When no symmetry is assumed we may find a spiral wave emanating at the center of the inlet plane and spiraling out (toward the wall) and down (toward the outlet).

Acknowledgment

Work supported by the U.S.-Israel Binational Science Foundation.

Notation

a_i = stoichiometric coefficient
a_v, A_v = interphase surface area per catalyst or reactor volume, respectively
C_{pf} = heat capacity of the fluid phase
D_e, D_{et} = effective axial dispersion coefficient and axial conductivity, respectively
h = heat transfer coefficient
ΔH = reaction enthalpy
k_c = mass transfer coefficient
L = reactor length
L_C, L_T = diffusion and conduction length scale, respectively
$p = du/d\chi$
t = dimensional time
V = interstitial fluid velocity
u, v = variables in the condensed model
u_+, u_i, u_- = upper, intermediate, and lower steady-state solutions
z = dimensional axial coordinate
z_{fi} = position of front i
$\langle\ \rangle$ = space average

Greek letters

ϵ_b = bed void fraction
ϵ, γ = ratio of time scales
δ = dimensionless diffusivity of the global variable
λ_0 = fluid variable feed value
ρ = density
θ^* = catalyst activity
θ_i = adsorbed layer concentration
τ_T, τ_C = thermal and concentration time scale, respectively

Subscripts

i = of species i
t, z = temporal and spatial derivatives, respectively
in = at the reactor inlet

Literature Cited

Adaje, J., and M. Sheintuch, "Comparison of Multiplicity Patterns of a Single Catalytic Pellet and a Fixed Catalytic Bed for Ethylene Oxidation," *Chem. Eng. Sci.*, **45**, 1331 (1990).

Arce, P., and D. Ramkrishna, "Pattern Formation in Catalytic Reactors: The Role of Fluid-Mixing," *AIChE J.*, **37**, 98 (1991).
Amariglio, A., O. Benali, and H. Amariglio, "Oscillatory Oxidation of Propene over Copper Oxides," *J. Catal.*, **118**, 164 (1989).
Bar, M., M. Eiswirth, H. H. Rotermund, and G. Ertl, "Solitary-Wave Phenomena in an Excitable Surface Reaction," *Phys. Rev. Lett.*, **69**, 945 (1992).
Bar, M., N. Gottschalk, M. Eiswirth, and G. Ertl, "Spiral Waves in a Surface Reaction: Model Calculations," *J. Chem. Phys.*, **100**(2), 1202 (1994).
Barelko, V. V., I. I. Kurochka, A. G. Merzhanov, and K. G. Shkadinski, "Investigation of Traveling Waves on Catalytic Wires," *Chem. Eng. Sci.*, **33**, 805 (1978).
Barkley, D., "A Model for Fast Computer Simulation of Waves in Excitable Media," *Physica D*, **49**, 61 (1991).
Barto, M., and M. Sheintuch, "Excitable Waves and Spatiotemporal Patterns in a Fixed-Bed Reactor," *AIChE J.*, **40**, 120 (1994).
Bell, J. C., N. I. Jaeger, and J. L. Hudson, "Coupled Oscillating Cobalt Electrodes," *J. Phys. Chem.*, **96**, 8671 (1992).
Boukalouch, M., J. Elezgray, A. Arneodo, J. Boissande, and P. De Kepper, "Oscillatory Instability Induced by Mass Interchange between Two Coupled Steady State Reactors," *J. Phys. Chem.*, **91**, 5843 (1987).
Brown, J. R., PhD Thesis, Univ. of Notre Dame, Notre Dame, IN (1985).
Brown, J. R., G. A. D'Netto, and R. A. Schmitz, "Spatial Effects and Oscillations in Heterogeneous Catalytic Reactions," *Temporal Order*, L. Rensing and N. Jaeger, eds., Springer-Verlag, p. 86 (1985).
Chang, H.-C., "The Domain Model for Heterogeneous Catalysis," *Chem. Eng. Sci.*, **38**, 535 (1983).
Chen, C. C., E. E. Wolf, and H. C. Chang, "Low-Dimensional Spatio-Temporal Thermal Dynamics on Nonuniform Catalytic Surfaces," *J. Phys. Chem.*, **97**(5), 1055 (1993).
Collin, P., and V. Bakakotaiah, "Modelling and Analysis of Moving Temperature Patterns on Catalytic Surfaces," *J. Chem. Phys.*, **101**(1), 814 (1994).
Cordonier, G. A., F. Schuth, and L. D. Schmidt, "Oscillations in Methylamine Decomposition on Pt, Rh, Ir: Experiments and Models," *J. Chem. Phys.*, **91**, 5374 (1989).
Cordonier, G. A., and L. D. Schmidt, "Thermal Waves in NH_3 Oxidation on a Pt Wire," *Chem. Eng. Sci.*, **44**(9), 1983 (1989).
Dawson, S. P., A. Lawniczak, and R. Kapral, "Interaction of Turing and Flow-Induced Chemical Instabilities," *J. Chem. Phys.*, **100**(7), 5271 (1994).
Dvorak, L., P. Pinkas, and M. Marek, "Dynamic Behavior of CO Catallytic Afterburner with Electric Heating," *Cat. Today*, **20**, 449 (1993).
Eigenberger, G., "On the Dynamic Behaviour of the Catalytic Fixed-Bed Reactor in the Region of Multiple-Steady States: I. The Influence of Heat Conduction in Two Phase Models," *Chem. Eng. Sci.*, **27**, 1909 (1972).
Ertl, G., "Oscillatory Catalytic Reactions at Single Crystal Surfaces," *Adv. Catal.*, **37**, 213 (1990).
Falcke, M., and H. Engel, "Influence of Global Coupling through the Gas Phase on the Dynamics of CO Oxidation on Pt(110)," *Phys. Rev. E*, **50**(2), 1353 (1994).
Fife, P. C., *Mathematical Theory of Reacting and Diffusing Systems*, Springer-Verlag, Berlin (1979).
Frank-Kamenetski, D. A., "Diffusion and Heat Transfer in Chemical Kinetics," 2nd ed., Plenum Press, New York (1969).
Froment, G. F., and K. B. Bischoff, *Chemical Reactor Analysis and Design*, 2nd ed., Wiley, New York (1990).
Gorodetskii, V., J. Lauterbach, H.-H. Rotermund, J. H. Block, and G. Ertl, "Coupling between Adjacent Crystal Planes in Heterogeneous Catalysis by Propagating Reaction Diffusion Waves," *Nature*, **370**, 276 (1994).
Graham, M. D., S. L. Lane, and D. Luss, "Proper Orthogonal Decomposition Analysis of Spatiotemporal Temperature Patterns," *J. Phys. Chem.*, **97**, 889 (1993a).
Graham, M. D., S. L. Lane, and D. Luss, "Temperature Pulse Dynamics on a Catalytic Ring," *J. Phys. Chem.*, **97**, 7564 (1993b).
Haim, D., O. Lev, L. M. Pismen, and M. Sheintuch, "Modelling Spatiotemporal Patterns in Anodic Nickel Dissolution," *Chem. Eng. Sci.*, **47**, 3907 (1992).
Hartmann, N., R. Imbihl, and W. Vogel, "Experimental Evidence for an Oxidation/Reduction Mechanism in Rate Oscillations of Catalytic CO Oxidation on Pt/SiO_2," *Cat. Lett.*, **28**, 373 (1994).
Hegedus, L. L., S. O. Oh, and K. Baron, "Multiple Steady States in an Isothermal, Integral Reactor: The Catalytic Oxidation of Carbon Monoxide over Platinum-Alumina," *AIChE J.*, **23**, 632 (1977).
Hefer, D., and M. Sheintuch, "Multiplicity Patterns of Inhomogeneous Solutions in Catalysts with Self-Inhibited Reactions," *Chem. Eng. Sci.*, **41**, 2295 (1986).
Hlavacek, V., and O. Van Rompay, "Current Problems of Multiplicity, Stability and Sensitivity of States in Chemically Reacting Systems," *Chem. Eng. Sci.*, **36**, 1587 (1981).
Hudson, J. L., J. Tabora, K. Krischer, and I. G. Kevrekidis, "Spatiotemporal Period Doubling during the Electrodissolution of Iron," *Phys. Lett. A*, **179**, 359 (1993).
Hudson, J. L., and T. T. Tsotsis, "Electrochemical Reactions Dynamics: A Review," *Chem. Eng. Sci.*, **49**, 1493 (1994).
Imbihl, R., "Oscillatory Surface Reactions," *Prog. Surf. Sc.*, **44**, 185 (1993).
Ivanova, A. N., "Multidimensional Stationary and Oscillating Regimes of Chemical Reactors," *Matematicheskiye Metody v Himicheskoi Kinetike*, "Nauka" (in Russian) (1990).
Jaeger, N. J., R. Ottensmeyer, and P. J. Plath, "Oscillations and Coupling Phenomena between Different Areas of the Catalyst during Heterogeneous Catalytic Oxidation of Ethanol," *Ber. Bunsenges. Phys. Chem.*, **90**, 1075 (1986).
Jakubith, S., H. H. Rotermund, W. Engel, A. von Oertzen, and G. Ertl, "Spatiotemporal Concentration Patterns in a Surface Reaction: Propagating and Standing Waves, Rotating Spirals and Turbulence," *Phys. Rev. Lett.*, **65**(24), 3013 (1990).
Jensen, K. F., and W. H. Ray, "A Microscopic Model for Catalytic Surfaces: 1. Catalytic Wires and Gauzes," **35**, 2439 (1980).
Jensen, K. F., and W. H. Ray, "The Bifurcation Behavior of Tubular Reactors," *Chem. Eng. Sci.*, **37**, 199 (1982a).
Jensen, K. F., and W. H. Ray, "A Microscopic Model for Catalytic Surfaces: 2. Supported Catalysts," **37**, 1387 (1982b).
Kapicka, J., and M. Marek, "Oscillations on Individual Catalytic Pellets in a Packed Bed," *J. Cat.*, **119**, 508 (1989).
Kaul, D. J., and E. E. Wolf, "FTIR Studies of Surface Reaction Dynamics: 1. Temperature and Concentration Programming during CO Oxidation on Pt/SiO_2," *J. Cat.*, **89**, 348 (1984).
Kim, S. H., and V. Hlavacek, "On the Detailed Dynamics of Coupled Continuous Stirred Tank Reactors," *Chem. Eng. Sci.*, **41**(11), 2767 (1986).
Kellow, J. C., and E. E. Wolf, "Propagation of Oscillations during Ethylene Oxidation on a Rh/SiO_2 Catalyst," *AIChE J.*, **37**, 1844 (1991).
Kellow, J. C., and E. E. Wolf, "Infrared Thermography and FTIR Studies of Catalyst Preparation Effects on Surface Reaction Dynamics during CO and Ethylene Oxidation on Rh/SiO_2," *Chem. Eng. Sci.*, **45**, 2597 (1990).
Kurtanjek, Z., M. Sheintuch, and D. Luss, "Surface State Kinetic Oscillations in the Oxidation of Hydrogen on Nickel," *J. Cat.*, **66**, 11 (1980).
Lane, L. L., M. D. Graham, and D. Luss, "Spatiotemporal Temperature Patterns during Hydrogen Oxidation on a Nickel Disk," *AIChE J.*, **39**, 1497 (1993).
Lauschke, G., and E. D. Giles, "Circulating Reaction Zones in a Packed-Bed Reactor," *Chem. Eng. Sci.*, **49**(24B), 5359 (1994).
Lauterbach, J., G. Haas, H. H. Rotermund, and G. Ertl, "Spatio-Temporal Pattern Formation on Polycrystalline Platinum Surfaces during Catalytic CO Oxidation," *Surf. Sci.*, **294**, 116 (1993).
Lauterbach, J., and H. H. Rotermund, "Spatial Pattern During Catalytic CO Oxidation on Pt(100)," *Surf. Sci.*, **311**, 231 (1994a).
Lauterbach, J., and H. H. Rotermund, "Gas-Phase Coupling in the CO-Oxidation on Polycrystalline Platinum," *Cat. Lett.*, **27**(12), 27 (1994b).
Lev, O., M. Sheintuch, L. M. Pismen, and H. Yarnitski, "Standing and Propagating Wave Oscillations in the Anodic Dissolution of Nickel," *Nature*, **338**, 458 (1988).
Lev, O., M. Sheintuch, L. M. Pismen, and H. Yarnitski, "Spatial Current Distribution during Nickel Anodic Dissolution in Sulfuric Acid," *Chem. Eng. Sci.*, **45**, 839 (1990).
Levine, H., and X. Zou, "Catalysis at Single-Crystal Pt(110) Surfaces: Global Coupling and Standing Waves," *Phys. Rev. E*, **48**, 50 (1993).
Lindstrom, T. H., and T. T. Tsotsis, "Reaction Rate Oscillations dur-

ing CO Oxidation over Pt/γ-Al_2O_3; Experimental Observations and Mechanistic Causes," *Surf. Sci.*, **150**, 487 (1985).
Lobban, L., and D. Luss, "Spatial Temperature Oscillations during Hydrogen Oxidation on a Nickel Foil," *J. Phys. Chem.*, **93**, 6530 (1989).
Lobban, L., G. Philippou, and D. Luss, "Standing Temperature Waves on Electrically Heated Catalytic Ribbons," *J. Phys. Chem.*, **93**, 733 (1989).
Meron, E., "Pattern Formation in Excitable Media," *Phys. Rep.*, **218**, 1 (1992).
Mertens, F., R. Imbihl, and A. Mikhailov, "Breakdown of Global Coupling in Oscillatory Surface Reaction," *J. Chem. Phys.*, **99**, 8668 (1993).
Middya, U., M. Sheintuch, M. D. Graham, and D. Luss, "Patterns of Temperature Pulses on Electrically Heated Catalytic Ribbons," *Physica D*, **63**, 393 (1993a).
Middya, U., M. D. Graham, D. Luss, and M. Sheintuch, "Patterns Selection in Controlled Reaction-Diffusion Systems," *J. Chem. Phys.*, **98**, 2823 (1993b).
Middya, U., D. Luss, and M. Sheintuch, "Spatiotemporal Motions Due to Global Interaction," *J. Chem. Phys.*, **100**, 3568 (1994a).
Middya, U., D. Luss, and M. Sheintuch, "Impact of Global Interactions and Symmetry on Pattern Selection and Bifurcation," *J. Chem. Phys.*, **101**, 4688 (1994b).
Mikhailov, A. S., *Foundations of Synergetics*, I: *Distributed Active Systems*, Springer-Verlag, Berlin (1991).
Oh, S. H., E J. Bisset, and P. A. Battison, "Mathematical Modeling of Electrically Heated Monolith Converters: Model Formulation, Numerical Methods, and Experimental Verification," *Ind. Eng. Chem. Res.*, **32**, 1560 (1993).
Onken, H. U., and E. Wicke, "Statistical Fluctuations of Temperature and Conversion at the Catalytic CO Oxidation in an Adiabatic Packed Bed Reactor," *Ber. Bunsenges Phys. Chem.*, **90**, 976 (1986).
Onken, H. U., and E. E. Wolf, "Coupled Chemical Oscillators on a Pt/SiO_2 Disk," *Chem. Eng. Sci.*, **43**, 2251 (1988).
Paspek, S. C., and A. Varma, "An Experimental and Theoretical Investigation of Ethylene Oxidation on Supported Platinum in an Adiabatic Fixed-Bed Reactor," *Chem. Eng. Sci.*, **35**, 33 (1980).
Philippou, G., M. Somani, and D. Luss, "Traveling Temperature Fronts on Catalytic Ribbons," *Chem. Eng. Sci.*, **48**, 2325 (1993).
Philippou, G., and D. Luss, "Temperature Patterns on a Catalytic Ribbon Heated by Constant Voltage," *Chem. Eng. Sci.*, **48**, 2313 (1993).
Philippou, G., and D. Luss, "Temperature Patterns on a Catalytic Ribbon Heated by a Constant Electric Current," *J. Phys. Chem.*, **96**, 6651 (1992).
Philippou, G., F. Shultz, and D. Luss, "Spatiotemporal Temperature Patterns on an Electrically Heated Catalytic Ribbon," *J. Phys. Chem.*, **95**, 3224 (1991).
Pismen, L. M., "Kinetic Instabilities in Man-Made and Natural Reactors," *Chem. Eng. Sci.*, **35**, 1950 (1980).
Plath, P. J., K. Muller, and N. I. Jaeger, "Cooperative Effects in Catalysis, Part 2.—Analysis and Modelling of the Temperature Dependence of the Oscillating Catalytic Oxidation of CO on a Palladium Al_2O_3-Supported Catalyst," *J. Chem. Soc., Faraday Trans. 1*, **84**, 1751 (1988).
Puszynski, J., and V. Hlavacek, "Experimental Study of Traveling Waves in Nonadiabatic Fixed Bed Reactors for the Oxidation of Carbon Monoxide," *Chem. Eng. Sci.*, **35**, 1769 (1980).
Puszynski, J., D. Snita, V. Hlavacek, and H. Hoffman, "A Revision of Multiplicity and Parametric Sensitivity Concepts in Nonisothermal Nonadiabatic Packed Bed Chemical Reactors," *Chem. Eng. Sci.*, **36**, 1605 (1981).
Puszynski, J., and V. Hlavacek, "Experimental Study of Ignition and Extinction Waves and Oscillatory Behaviour of a Tubular Nonadiabatic Fixed Bed Reactor for the Oxidation of Carbon Monoxide," *Chem. Eng. Sci.*, **39**, 681 (1984).
Qin, F., E. E. Wolf, and H. C. Chang, "Controlling Spatiotemporal Patterns on a Catalytic Wafer," *Phys. Rev. Lett.*, **72**(10), 1459 (1994).
Qin, F., and E. E. Wolf, "Vibrational Control of Chaotic Self-sustained Oscillations during CO Oxidation on a Rh/SiO_2 Catalyst," *Chem. Eng. Sci.*, **50**, 117 (1994).
Razon, L. F., and R. A. Schmitz, "Multiplicities and Instabilities in Chemically Reacting Systems," *Chem. Eng. Sci.*, **42**, 1005 (1987).
Rehacek, J., M. Kubicek, and M. Marek, "Modelling of a Tubular Catalytic Reactor with Flow Reversal," *Chem. Eng. Sci.*, **47**, 2897 (1992).
Rhee, H.-K., R. P. Lewis, and N. R. Amundson, "Creeping Profiles in Catalytic Fixed-Bed Reactors. Continuous Models," *Ind. Eng. Chem. Fundam.*, **13**, 317 (1974).
Rhee, H.-K., D. Foley, and N. R. Amundson, "Creeping Reaction Zone in a Catalytic Fixed-Bed Reactors: A Cell Approach," *Chem. Eng. Sci.*, **28**, 707 (1973).
Rotermund, H. H., "Investigation of Dynamic Processes in Adsorbed Layers by Photoemission Electron Microscopy," *Surf. Sci.*, **283**, 87 (1993).
Rovinsky, A. B., and M. Menzinger, "Chemically Instability Induced by a Differential Flow," *Phys. Rev. Lett.*, **69**, 1139 (1992).
Rovinsky, A. B., and M. Menzinger, "Self-Organization Induced by Differential Flow of Activator and Inhibitor," *Phys. Rev. Lett.*, **70**, 778 (1993).
Sangalli, M., and H.-C. Chang, "Complex Spatiotemporal Motions in an Open Flow Reactor," *Phys. Rev. E*, **49**, 5207 (1994).
Sant, R., and E. E. Wolf, "FTIR Studies of Catalyst Preparation Effects on Spatial Propagation of Oscillations during CO Oxidation on Pt/SiO_2," *J. Cat.*, **110**, 249 (1988).
Schmitz, R. A., and T. T. Tsotsis, "Spatially Patterned States in Systems of Interacting Catalyst Particles," *Chem. Eng. Sci.*, **38**, 1431 (1983).
Schuth, F., X. Song, L. D. Schmidt, and E. Wicke, "Synchrony and the Emergence of Chaos in Oscillations on Supported Catalysts," *J. Chem. Phys.*, **92**, 745 (1990).
Schuth, F., B. E. Henry, and L. D. Schmidt, "Oscillatory Reactions in Heterogeneous Catalysis," *Adv. Cat.*., **39**, 51 (1993).
Sharma, C. S., and R. Hughes, "The Behaviour of an Adiabatic Fixed Bed Reactor for the Oxidation of Carbon Monoxide: II. Effect of Perturbations," *Chem. Eng. Sci.*, **34**, 625 (1979).
Sheintuch, M., and R. A. Schmitz, "Oscillations in Catalytic Reactions," *Catal. Rev.—Sci. Eng.*, **15**(1), 107 (1977).
Sheintuch, M., and L. M. Pismen, "Inhomogeneities and Surface Structures in Oscillatory Catalytic Reactions," *Chem. Eng. Sci.*, **36**, 489 (1981).
Sheintuch, M., and J. Schmidt, "Observable Multiplicity Features of Inhomogeneous Solutions Measured by the Thermochemic Method, Theory and Experiments," *Chem. Eng. Commun.*, **44**, 35 (1986).
Sheintuch, M., "The Determination of Global Solutions from Local Ones in Catalytic Systems Showing Steady-State Multiplicity," *Chem. Eng. Sci.*, **42**, 2103 (1987).
Sheintuch, M., and D. Hefer, "Dynamic Behaviour of Inhomogeneous Solutions in Catalysts with Self-Inhibited Reactions," *Chem. Eng. Sci.*, **43**, 519 (1988).
Sheintuch, M., "Spatiotemporal Structures of Controlled Catalytic Wires," *Chem. Eng. Sci.*, **44**, 1081 (1989a).
Sheintuch, M., "Kinetics Falsification by Symmetry Breaking. 1. Steady State Analysis," *Ind. Eng. Chem. Res.*, **28**, 948 (1989b).
Sheintuch, M., and J. Adjaye, "Excitable Waves in a Fixed-Bed Reactor: Ethylene Oxidation on Platinum," *Chem. Eng. Sci.*, **45**, 1897 (1990).
Sheintuch, M., "Excitable Waves in a Fixed-Bed Reactor: Observations and Analysis," *Chem. Eng. Sci.*, **45**, 2125 (1990a).
Sheintuch, M., "Numerical Approaches for Computation of Fronts," *Numer. Methods Partial Differ. Eqs.*, **6**, 43 (1990b).
Sheintuch, M., and S. Shvartsman, "Patterns Due to Convection-Conduction-Reaction Interaction in a Fixed-Bed Reactor," *Chem. Eng. Sci.*, **49**(24b), 5315 (1994).
Shvartsman, S., and Sheintuch, "Spatiotemporal Patterns in an Isothermal Heterogeneous Fixed-Bed Reactor," *J. Chem. Phys.*, **101**, 9573 (1994).
Shvartsman, S., and M. Sheintuch, "One- and Two-Dimensional Spatiotemporal Thermal Patterns in a Fixed-Bed Reactor," *Chem. Eng. Sci.*, **50**, 3125 (1995).
Simon, D., and D. Vortmeyer, "Measured and Calculated Migration Speeds of Reaction Zones in a Fixed Bed Reactor, A Quantitative Comparison," *Chem. Eng. Sci.*, **33**, 109 (1978).
Slinko, M. M., and N. J. Jaeger, *Oscillatory Heterogenous Catalytic Systems*, Studies in Surface Science and Catalysis, Vol. 86, Elsevier, New York (1994).
Tsai, P. K., M. B. Maple, and K. H. Herz, "Coupled Catalytic Oscil-

lators: CO Oxidation over Polycrystalline Pt," *J. Catal.*, **113**, 4335 (1988).
Turing, A. M., "The Chemical Basis for Morphogenesis," *Phil. Trans. R. Soc.*, **B237**, 37 (1952).
Turner, J. E., B. C. Sales, and M. B. Maple, "Oscillatory Oxidation of CO on Pd and Ir Catalysts," *Surf. Sci.*, **109**, 591 (1981).
Vayenas, C. G., B. Lee, and J. Michaels, "Kinetics, Limit Cycles, and Mechanisms, of Ethylene Oxidation on Platinum," *J. Catal.*, **66**, 36 (1980).
Veser, G., and R. Imbihl, "Synchronization and Spatiotemporal Organization in the NO+CO Reaction on Pt(100): II. Synchronized Oscillations on the Hex-Substrate," *J. Chem. Phys.*, **100**, 8492 (1994).
Volodin, Yu. E., V. N. Zvyagin, A. N. Ivanova, and V. V. Barelko, "On the Theory of the Origin of Spatially Nonuniform Stationary States (Dissipative Structures) in Heterogeneous Catalytic Systems," *Adv. Chem. Phys.*, **77**, 51 (1990).
Votruba, J., and V. Hlavacek, "Experimental Study of Multiple States in a Tubular Adiabatic Reactor," *Int. Chem. Eng.*, **14**, 461 (1974).
Wang, Y., and J. L. Hudson, "Experiments on Interacting Electrochemical Oscillators," *J. Phys. Chem.*, **96**, 8667 (1992).
Wedel, S., and D. Luss, "Steady State Multiplicity Features of an Adibatic Fixed-Bed Reactor with Langmuir-Hinshelwood Kinetics, CO or CO_2 Methanation," *Ind. Eng. Chem. Fundam.*, **23**, 280 (1984).
Wicke, E., and D. Vortmeyer, "Zudzonen heterogener Reaktionen in gasdurchstromten Kornerschichten," *Z. Elektochem. Ber. Bunsenges. Phys. Chem.*, **63**, 145 (1959).
Wicke, E., and H. U. Onken, "Periodicity and Chaos in a Catalytic Packed Bed Reactor for CO Oxidation," *Chem. Eng. Sci.*, **43**, 2289 (1988).
Yakhnin, V. Z., A. B. Rovinsky, and M. Menzinger, "Differential-Flow-Induced Pattern Formation in the Exothermic A → B Reaction," *J. Phys. Chem.*, **98**, 2116 (1994).
Yakhnin, V. Z., A. B. Rovinsky, and M. Menzinger, "Convective Instability Induced by Differential Transport in the Tubular Packed Bed Reactor," *Chem. Eng. Sci.*, submitted (1995).
Zhdanov, V. P., "Kinetic Model of the Hydrogen-Oxygen Reaction on Platinum: Bistability, Chemical Waves and Oscillations," *Surf. Sci.*, **296**, 261 (1993).

Manuscript received Feb. 7, 1995, and revision received June 17, 1995.